REPORT DOCUMENTATION PAGE

Form Approved
OMB No. 0704-0188

1. REPORT DATE *(DD-MM-YYYY)*	2. REPORT TYPE	3. DATES COVERED *(From - To)*
04-10-2009	Journal Article	

4. TITLE AND SUBTITLE

Storm-Generated Sediment Distribution along the Northwest Florida Inner Continental Shelf

5a. CONTRACT NUMBER

5b. GRANT NUMBER

5c. PROGRAM ELEMENT NUMBER

6. AUTHOR(S)

W. Chad Vaughan, Kevin B. Briggs, Jin-Wook Kim, Thomas S. Bianchi, and Richard W. Smith

5d. PROJECT NUMBER

5e. TASK NUMBER

5f. WORK UNIT NUMBER

74-7632-07

7. PERFORMING ORGANIZATION NAME(S) AND ADDRESS(ES)

Naval Research Laboratory
Marine Geoacoustics Division
Stennis Space Center, MS 39529

8. PERFORMING ORGANIZATION REPORT NUMBER

NRL/JA/7430-07-11

9. SPONSORING/MONITORING AGENCY NAME(S) AND ADDRESS(ES)

Office of Naval Research
800 North Quincy Street
Arlington VA 22217-5000

10. SPONSOR/MONITOR'S ACRONYM(S)

ONR

11. SPONSOR/MONITOR'S REPORT NUMBER(S)

12. DISTRIBUTION/AVAILABILITY STATEMENT

Approved for public release; distribution is unlimit

13. SUPPLEMENTARY NOTES

0-933957-38-1 2009 MTS

Abstract—**Hurricane Ivan made landfall along the Alabama–Florida coastline on September 16, 2004 as a category 3 storm. Ivan provided a rare opportunity to quantify surficial sediment changes following a significant storm event. Sidescan sonar imagery was collected immediately offshore Santa Rosa Island, FL, five days before and after Ivan's landfall 100 km west of the study area. Particle-size, multisensor core logger, X-radiography, photography, scanning electron microscopy (SEM) grain shape, direct shear, radiocarbon isotope, and lignin–phenol analyses were performed on grab or vibracore samples collected after the storm. Sonar observations before Ivan's landfall revealed a mostly sand bottom with uniform, small-scale wind-wave ripple morphology, and a distinct area of low backscatter trending NW–SE that was interpreted to be a mud swale. Ivan introduced new material to the relict sediments and resulted in the deposition of fine-grained material across the shelf that settled in the bathymetric lows and formed mud flaser deposits. Hardbottoms were draped by sand in some locations, but exposed in others. Ripple morphology changes occurred along sand ridges. Hurricane Ivan created major sediment distribution changes along the near-shore shelf, yet served to reinforce and to maintain the ridge-and-swale topography of the northeastern Gulf of Mexico near-shore continental shelf.**

15. SUBJECT TERMS

Lignin, seafloor imagery, sedimentation, sediments

16. SECURITY CLASSIFICATION OF:			17. LIMITATION OF ABSTRACT	18. NUMBER OF PAGES	19a. NAME OF RESPONSIBLE PERSON
a. REPORT	b. ABSTRACT	c. THIS PAGE			Kevin Briggs
Unclassified	Unclassified	Unclassified	UU	21	19b. TELEPHONE NUMBER *(Include area code)* 228-688-5518

Storm-Generated Sediment Distribution Along the Northwest Florida Inner Continental Shelf

W. Chad Vaughan, Kevin B. Briggs, Jin-Wook Kim, Thomas S. Bianchi, and Richard W. Smith

Abstract—**Hurricane Ivan made landfall along the Alabama–Florida coastline on September 16, 2004 as a category 3 storm. Ivan provided a rare opportunity to quantify surficial sediment changes following a significant storm event. Sidescan sonar imagery was collected immediately offshore Santa Rosa Island, FL, five days before and after Ivan's landfall 100 km west of the study area. Particle-size, multisensor core logger, X-radiography, photography, scanning electron microscopy (SEM) grain shape, direct shear, radiocarbon isotope, and lignin–phenol analyses were performed on grab or vibracore samples collected after the storm. Sonar observations before Ivan's landfall revealed a mostly sand bottom with uniform, small-scale wind-wave ripple morphology, and a distinct area of low backscatter trending NW–SE that was interpreted to be a mud swale. Ivan introduced new material to the relict sediments and resulted in the deposition of fine-grained material across the shelf that settled in the bathymetric lows and formed mud flaser deposits. Hardbottoms were draped by sand in some locations, but exposed in others. Ripple morphology changes occurred along sand ridges. Hurricane Ivan created major sediment distribution changes along the near-shore shelf, yet served to reinforce and to maintain the ridge-and-swale topography of the northeastern Gulf of Mexico near-shore continental shelf.**

Index Terms—**Lignin, seafloor imagery, sedimentation, sediments.**

I. Introduction

EPISODIC tropical storm events in the northern Gulf of Mexico often shape the continental shelf seabed. For instance, strong tropical events can be preserved in the near-shore seabed by event layering resulting from the mobilization, entrainment, resuspension, and redeposition of sediment due to the physical force of these storms. Typical of storm sedimentation preserved in the seabed are coarse lag layers, fining-upward sequences, and hummocky cross stratification [1]. The impact of strong tropical systems on muddy near-shore and estuarine environments of the northern Gulf, specifically the preservation of sandy event layers, is documented [2]–[4]. The uniformity of sand and the shallow water along the northeastern Gulf and the Florida Panhandle shelf may make long-term preservation of event layers much less likely. However, tropical systems are known to cause large disruptions to fine-grained estuarine and back-barrier environments along the northern Gulf that result in outflow of sediment to the offshore as well as washover fans into the lagoon [5]–[8].

Hurricane Ivan made landfall along the Alabama–Florida coastline on September 16, 2004 as a category 3 storm on the Saffir–Simpson hurricane scale (SSHS). The timing and location of Ivan's landfall provided an excellent opportunity to document surficial sediment changes following a significant storm event. As part of the U.S. Office of Naval Research program to investigate the influence of sediment heterogeneity on coastal dynamics, sidescan sonar data were collected within a 6-km^2 area along the Florida Panhandle within 1 km offshore of the Santa Rosa Island barrier beach in 3–21 m of water before Ivan's landfall (Fig. 1). The site lies offshore a 90-m-high observation tower that is one location for the Video Imaging System for Surf Zone Environmental Reconnaissance (VISSER), a system of worldwide surf zone video imaging sites operated by the U.S. Naval Research Laboratory (NRL). These imaging sites provide hydrodynamic and morphodynamic information from automated image processing techniques. The sidescan sonar survey was conducted in view of the VISSER system to provide sediment distribution information for the "Coastal Dynamics in Heterogeneous Sedimentary Environments" basic research initiative at NRL. In addition, the survey was conducted concomitantly with the 2004 Sediment Acoustics Experiment (SAX04), which was conducted September–November 2004, 11 km to the east in similar water depths. The area south of the VISSER tower was resurveyed and grab and vibracore samples for ground-truthing were collected after Ivan's landfall to observe the poststorm redistribution of sediment types within this study area.

For a storm to cause a major disruption of bottom sediments in estuaries and bays several characteristics are required, including: 1) a storm path to the west of the bay, 2) strong sustained wind speed, 3) long duration of high storm surge, 4) occurrence during normal high tide, and 5) slow passage [6]. Santa Rosa Island and its back-barrier lagoon and adjacent bays likely experienced each of these conditions as Hurricane Ivan passed just to the west, produced Category 3 wind speeds, and a 3.0–4.5-m storm surge near the time of the National Oceanic and Atmospheric Administration's predicted mean higher high water at Pensacola.[1] Thus, Hurricane Ivan could be expected to

Manuscript received October 01, 2007; revised August 11, 2008; accepted January 14, 2009. First published August 04, 2009; current version published November 25, 2009. This work was supported by the U.S. Office of Naval Research and the U.S. Naval Research Laboratory (NRL) Program Element 0601153N. The NRL contribution number is JA/7430-07-11.

Associate Editor: M. D. Richardson.

W. C. Vaughan was with the Naval Research Laboratory, Stennis Space Center, MS 39529 USA. He is now with the Minerals Management Service, New Orleans, LA 70123 USA (e-mail: Chad.Vaughan@mms.gov).

K. B. Briggs is with the Naval Research Laboratory, Stennis Space Center, MS 39529 USA.

J.-W. Kim was with the Naval Research Laboratory, Stennis Space Center, MS 39529 USA. He is now with Yonsei University, Seoul 120-749, South Korea.

T. S. Bianchi and R. W. Smith are with Texas A&M University, College Station, TX 77843 USA.

Digital Object Identifier 10.1109/JOE.2009.2014660

[1]http://tidesandcurrents.noaa.gov/

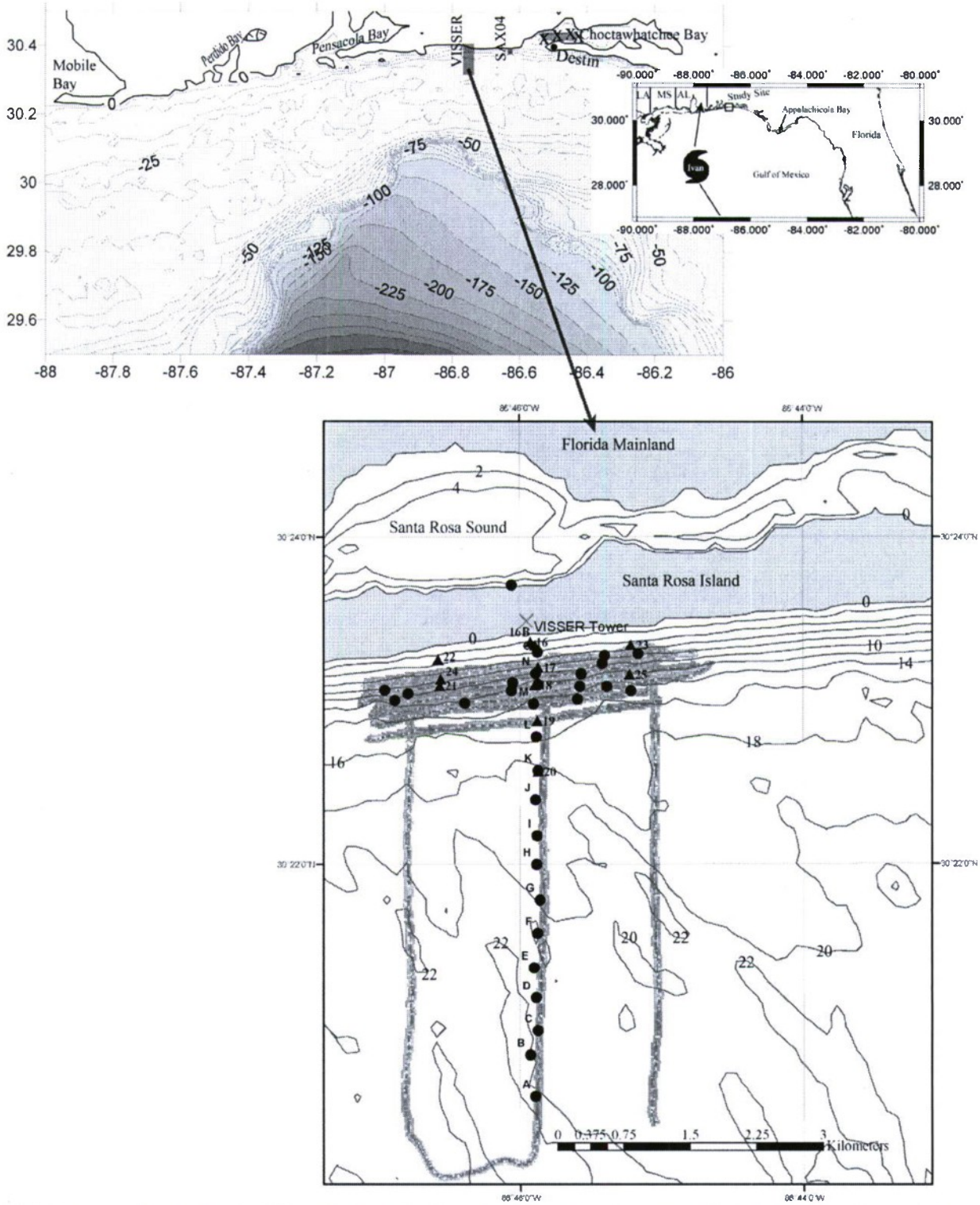

Fig. 1. Gulf of Mexico site maps along the NW Florida Panhandle. The small-scale map shows the general path of Hurricane Ivan. The sampled areas of the VISSER, SAX04, and Choctawhatchee Bay sites are shadowed in gray in the midscale map. The SAX04 experiment site is about 11 km to the east of the VISSER site, and the Choctawhatchee Bay samples are an additional 12–22 km to the east inside the Bay. Each location of the four grab samples in Choctawhatchee Bay is marked by an X on the midscale map and named CBay1–4 in the east to west direction. The VISSER tower is marked by the X on the large-scale map, with sidescan sonar tracklines shadowed in gray and grab samples as circles and vibracores as triangles. NOAA Coastal Relief Model bathymetry is shown with 5-m contour intervals in the midscale map until the 100-m depth contour where the interval changes to 25 m. The VISSER site map bathymetry is contoured at 2-m intervals and shows the ridge-and-swale topography of the region.

cause sediment dispersal to the continental shelf and influence sediment distribution along the near-shore Gulf shelf.

This paper discusses the effects of a major storm event on sediment distribution in the near-shore environment with a

goal to map the sediment distribution with acoustic imagery and ground-truth the imagery with sediment sampling. Our larger objective is to determine large-scale sediment horizontal distribution and vertical heterogeneity (substrate thickness) from a near-shore environment in the Gulf of Mexico; especially to characterize event-driven (storm-generated) changes in sediment distribution and heterogeneity and relate it to the physical forcing and sediment properties. A secondary objective is to provide a regional geologic context for geoacoustic measurements conducted during SAX04.

II. Physical Description

A. Regional Geologic Setting

The study site lies along the northwest Florida Panhandle inner continental shelf, the east flank of the Mississippi embayment, and the Gulf Coast Geosyncline. The shelf in this region is wide, low gradient, and low energy. Thick terrigenous clastic sequences have accumulated beneath the Alabama–Florida Shelf since Miocene to Recent times [9]. Modern surface sediments in this area, referred to as the Mississippi–Alabama–Florida (MAFLA) sand sheet lie within the Eastern Gulf Province, a sediment province that stretches east along the shelf from the abandoned St. Bernard delta lobe to the Apalachicola delta [10]–[12].

Numerous investigations have concentrated on the Neogene to Recent shelf geology, including the Late Pleistocene geology and Holocene surficial sediments of the northwestern Florida shelf, especially the morphologic and stratigraphic signatures of the last eustatic sea-level rise [13]–[19]. Our study area lies within the Eastern Gulf Province, and within the shore-parallel geomorphic zone dominated by shore-oblique (70°) shelf and shoreface-connected sand ridges [20], [21]. A combination of pretransgressive, transgressive, and post-transgressive processes have served to superimpose higher order Holocene features over first-order Pleistocene features [22]. These surficial features include shore-perpendicular bathymetric lows, shelf-edge lobes, shore-parallel long linear shoals and bathymetric lows, and shore-oblique shelf and shoreface sand ridges.

Six primary sedimentary facies characterize the last eustatic sea-level rise in the northeastern Gulf shelf subbottom for the transgressed MAFLA shelf [17], [19]. During the Late Quaternary (Wisconsin) sea-level drop approximately 18 000 years before present (B.P.), the drainage systems of northwest Florida cut across the shelf forming bathymetric lows and shelf-edge delta lobes. Shore-perpendicular bathymetric lows in the region likely result from fluvial systems in response to the glacio–eustatic sea-level fall. Linear shoals southwest of the study area at the 25- and 35-m isobaths suggest former barrier shoreline positions during sea-level lowstands around 7000 and 11 000 years B.P., respectively. However, the shoals themselves probably relate to transgressive and post-transgressive processes rather than actual barrier sedimentary deposits since their preservation is unlikely as the sediments lie above a shoreface ravinement, and open marine species dominate the foraminiferal and molluscan assemblages [19]. Erosional retreat of the shoreline during the transgression draped a trailing sand sheet over the transgressive topography. Post-transgressive processes, such as tide, wind, current, and storm events, reworked the sand shelf once sea level reached its present day shoreline 6000 to 3000 years B.P. Thus, the last fall and subsequent rise in eustatic sea level greatly influenced the surface morphology of the northeastern Gulf [22], [23].

Eastern Gulf Province sediments are fluvial in origin. However, the sedimentologic dominance of the Mississippi River diminishes with distance east of the Louisiana shelf. Eastern Gulf sands have an Appalachian origin based on mineralogy [12]. Therefore, the major sediment suppliers are the Mobile River to the west of the study area and the Apalachicola River to the east. The Florida Panhandle shelf is restricted from Mobile Bay sediment due to the net long-shore currents [22], [24]. A subtle, yet distinct east-to-west size and sorting trend exists from moderately sorted, medium-grained quartz sand to moderately well-sorted, fine-grained quartz sand. There is a sharp sedimentologic boundary between the Mobile and Apalachicola subprovinces 25 km west offshore Perdido Bay [22].

Clay and heavy mineral assemblages, grain size, and grain shape further indicate that the Eastern Gulf Province sediments are dominated by the Apalachicola River and other rivers of the southeastern United States [11], [13], [14], [24]. Seismic studies show that the Perdido, Escambia, Choctawhatchee, and Apalachicola River systems incised a network of channels on the continental shelf during the Late Quaternary lowstand with the Apalachicola being larger than any of its modern day counterparts with significantly larger discharge. Although the modern Apalachicola River deposits its sediment load in a shallow estuary (Apalachicola Bay) further to the east, it likely was the dominant supplier of sediment to this shelf area and the probable source of coastal sands of the Florida Panhandle shelf when it was as much as twice its current size [10], [15], [25]. Thus, the study area along the near-shore Panhandle shelf contains palimpsest sediments delivered by the Apalachicola River system during the last fall and subsequent rise in eustatic sea level and mostly reworked during the Pleistocene.

The sediments are fine- to medium-grained quartz sand that generally fine westward in the direction of the net long-shore sediment transport. Sediments along the beaches have been described as having a strikingly uniform texture, composed predominantly of quartz with few accessory minerals [10], [22], [26]. The source of these quartz sediments along the eastern half of Santa Rosa Island is an eroding Pleistocene "headland" east of Destin [27]. Moreover, Recent beach sands are similar to the Pleistocene sands in grain size and mineralogy. Hence, the beach sands of the study area and of northwest Florida were likely derived by the reworking of older Pleistocene sediments, and not transported from the modern Apalachicola River [26].

B. Santa Rosa Island and Santa Rosa Sound

Santa Rosa Island is a narrow, low-profile, dune, and washover barrier island of Holocene origin approximately 80 km in length. The island is about 500 m in width adjacent to the study area and is bounded by the Pensacola Bay to the west, Choctawhatchee Bay to the east, the Gulf of Mexico to the south, and Santa Rosa Sound to the north separating the barrier island from the Florida Panhandle mainland. Santa Rosa Sound is a shore-parallel lagoon approximately 0.4 km wide and up to

7.5 m deep. The Santa Rosa Island core evolved during marine transgression and is composed of Late Pleistocene barrier deposits underlain by the Pleistocene Biloxi Formation, which is composed of open near-shore and brackish water deposits. This Pleistocene core at no point rises above present mean sea level on the island, and was submerged during the transgression and overlain by Holocene shoreface, beach, and dune deposits [16]. Most of the island has maintained relative historical stability [28].

Santa Rosa Island is part of a barrier island complex separating a series of lagoons, bays, and estuaries from the Gulf of Mexico. These estuaries north of the barrier islands are sinks for fine-grained sediment, and little sediment is transported to the Gulf except from the Mobile Bay plume or during hurricane events [5]–[7], [29]–[31].

C. Hurricane Ivan

Hurricane Ivan made landfall just west of Gulf Shores, Alabama on the morning of September 16, 2004 as a Category 3 storm. This was approximately 100 km west of our study area. Persistent maximum wind speeds were highest in the outermost concentric eyewall of the northeastern quadrangle for several hours before landfall. The 50-nmi-diameter eyewall resulted in a maximum recorded Doppler radar wind speed of 54 m/s 72 km west of our study area. Geographically, the study area lies between the officially recorded sustained surface wind speeds of 39.1 m/s with 47.8-m/s gusts at the Pensacola Naval Air Station and 30.9-m/s winds with gusts of 39.6 m/s at the Destin Airport [32].

The National Data Buoy Center's (NDBC) buoy 42040 (64 nmi south of Dauphin Island, AL) recorded a significant wave height of 15.96 m, the largest ever reported by the NDBC (until the following year when the same buoy recorded a significant wave height of 16.91 m during Hurricane Katrina) [33]. Wave-tide gauges deployed near this buoy by the Naval Research Laboratory, Stennis Space Center, MS, measured wave heights up to 17.9 m during Ivan, as well as the largest maximum individual wave height of 27.7 m [34]. These measurements were recorded while Hurricane Ivan was still classified as a Category 4 storm as it approached the outer continental shelf.

Although Hurricane Ivan underwent weakening as it came onshore, the storm resulted in a 3.0–4.5-m storm surge in the study area [32]. Aerial reconnaissance immediately after Ivan indicates that at least a portion of Santa Rosa Island was completely submerged. Moderate-resolution imaging spectroradiometer (MODIS) imagery reveals estuarine sediment discharge plumes in the Gulf following the storm, including plumes from Pensacola and Choctawhatchee Bays on either side of the study area [8].

III. Methods

A. Acoustic Surveys

Sidescan sonar data was collected using a Marine Sonic Technology, Ltd. (White Marsh, VA), 300-kHz system with PC-Windows-based Sea Scan PC software for data acquisition. Raw data files were processed using Chesapeake Technology, Inc. (Mountain View, CA), SonarWeb Pro software to create sonar mosaics and waterfall imagery. The survey conducted parallel to shore was aborted due to Hurricane Ivan's approach, and repeated five days after landfall. Three additional poststorm track lines were surveyed perpendicular to shore to about 6 km offshore: one in line with the VISSER tower, and two at each edge of the survey box. The surveys were conducted aboard the *R/V Pelican*, a 35-m research vessel operated by the Louisiana Universities Marine Consortium (LUMCON), in water depths as shallow as allowed by the vessel's 3-m draft and within the surf zone. Thus, short cable-out lengths and wave conditions created distinct artifacts in some of the sonar data as a result of vessel heave. These artifacts are particularly prominent in data collected in the shallow-water areas.

A multibeam survey of the area was conducted by the University of New Hampshire Center for Coastal and Ocean Mapping/Joint Hydrographic Center, Durham, on September 3, 2004 about two weeks before Hurricane Ivan's landfall and again in October 2004, 41 days after Hurricane Ivan made landfall. The high-resolution multibeam backscatter data were collected with a 300-kHz Kongsberg Maritime (Kongsberg, Norway) EM3002 system, and the imagery was draped over 455-kHz Reson 8125 bathymetry at a 25-cm grid [35].

B. Sediment Sampling

Fifteen grab samples were collected at select locations based on a preliminary analysis of the poststorm sidescan data. Fifteen additional grab samples, labeled A through O in the inshore direction, were collected in a shore-normal transect in line with the VISSER tower in 21-m water depth at 5 km offshore to 4.7-m water depth at 300 m offshore the island beach. Grab samples were collected using a Smith–McIntyre grab sampler. Eleven additional samples were manually collected on the beach from the base of the VISSER tower into the swash zone and one sample was collected in the lagoon behind the VISSER tower in August 2005. Also, four grab samples were collected in eastern Choctawhatchee Bay with a PONAR grab sampler in January 2007 and sand samples were manually collected by divers at six of the locations along the shore-normal transect in February 2007. Each sample was bagged and stored in a cooler until transported to the laboratory for particle-size analysis.

Twenty-six vibracores were collected in July and August 2005, eleven offshore the VISSER tower site and fifteen from the nearby SAX04 site. The vibracores were collected aboard the U.S. Geological Survey (USGS) *R/V Gilbert* using 7.6-cm diameter, 6-m length aluminum barrels attached to a pneumatic Rossfelder vibrator. Core recovery length varied between 0.67 and 5.6 m, and averaged 3.4 m. Five of those vibracores (16–20) were collected in line with the VISSER tower in water depths between 3.5 and 18 m, essentially along the shore-perpendicular sidescan trackline and the grab sample transect in the center of the survey box.

C. Sediment Laboratory Analysis

The vibracores were transported to the laboratory and logged at 1-cm intervals with an automated Geotek Limited (Daventry, U.K.) multisensor core logger. The logger obtained gamma-ray-attenuated sediment bulk density data with a

3.7×10^8-Bq Cs-137 gamma radiation source at energies of 0.662 MeV and compressional (P-wave) speed data with a 500-kHz transducer/receiver recording directly through the core liner. Acoustic impedance was calculated as the product of the density and P-wave speeds, and fractional porosity was estimated assuming a grain density of 2.65 g/cm^3.

P-wave speed measurements proved difficult to measure due to a low signal-to-noise ratio (SNR) of the received acoustic signal. The attenuated signal was a result of the aluminum liners in which the sediment was collected by the vibracorer, as well as the shell fragments that allowed for disruption of sediment fabric inside the cores. Moreover, some cores may have experienced drainage during transportation as indicated by drying of the sediment near the top of the cores. Consequently, speed data were "thinned" by removing all data where the relative amplitude fell below 50 on a log scale of 100, and speeds that were less than 1450 m/s. The relative amplitude is defined by a minimum and maximum voltage setting, and the relative value of 50 at the defined settings represents the level at which the electronics loses the ability to pick a timing pulse. Despite the discontinuous record of P-wave speed and impedance values due to data rejection, the data values are still valid as a relative measurement of acoustic trends within or between cores.

X-radiographs were collected using a Faxitron X-Ray, LLC (Lincolnshire, IL) 43855C system with a digital EZ40M line scanner. Because individual scans span approximately 25 cm in length, each scan was merged with its adjacent scan to construct a single 0.5-m length X-radiograph. Upon obtaining the X-radiograph images, each core was split into two halves: one half was photographed and archived, and the second half was sampled at 20-cm intervals (in addition to sampling of visually apparent sediment facies) for grain size analysis.

Sediment grain size analysis was conducted on each grab sample and vibracore subsample, using the grain size classification based on [36] and standard sieve and pipette procedures described in detail in [37]. In brief, the wet samples were sieved through a 62-μm screen to separate the coarse (sand- and gravel-sized) fraction from the fine (silt- and clay-sized) fraction. The fine fraction was collected in a 1000-mL cylinder of dispersant. Each coarse fraction was analyzed at quarter-phi intervals (Krumbein scale) with the sand- and gravel-fraction passing through a series of sieves on a sieve shaker. The silt and clay fractions were separated via a pipette aliquot from the fine fraction contained in suspension. When significant amounts of mud were present (generally >5% by [dry] weight), the complete mud fraction was analyzed using a Micromeritics (Norcross, GA) Sedigraph Model 5120 that employs X-ray absorption to determine the particle size distribution for particles finer than 63 μm in an aqueous suspension. Pipette aliquots were also collected at the 11- and 12-phi intervals for those samples analyzed with the Sedigraph.

D. Grain Shape Analysis

To attain knowledge of cumulative, long-term processes transporting the shelf sediments off Santa Rosa Island, we examined the grain shape of a spatially separated series of sand samples utilizing a scanning electron microscope (SEM) equipped with an integrated software package "EDS 2006" by IXRFsystems, Inc. (Houston, TX). Grain shape parameters were compared for sand grains from grabs collected along the VISSER tower transect in 2004 and 2007. In addition, two samples from a sectioned diver core collected at the nearby SAX04 site were analyzed for grain shape.

1) Scanning Electron Microscopy: Sample preparation is critical to obtain the optimum resolution by SEM for investigating grain shape. A total of 60–120 grains from seven locations (A, C, G, J, L, M, and the base of the VISSER tower) were selected for resin embedding. The sediment samples were cleaned, dried, and encased in epoxy (Bondo) resin. Well-defined contact between grain boundary and resin is necessary for the grain shape image analysis by SEM micrographs. Bondo epoxy resin, to our best knowledge, yields a superior grain boundary compared with L. R. White/Nanoplast resin. After curing for 8 h at room temperature, sample mounts were ground down to intercept the sand grains and then polished with a decreasing sequence of corundum grit, ultimately reaching 0.3-μm grit size. The samples were cleaned in an ultrasonic bath for 2 min and then transferred to an oven at 60 °C for drying overnight. The samples were coated with 250 Å of carbon under a vacuum of 0.00133 Pa. A digital AMRAY 1820 SEM was operated at an acceleration potential of 15 kV, a working distance of 18 mm, a sample tilt of 0°, and a final aperture size of 400 μm at the Electron Microscopy Laboratory, University of New Orleans, New Orleans, LA.

2) Image Analysis: SEM images were captured via the integrated software package "EDS 2006" at a resolution of 512 x 512 pixels and using an average of 16 screen renderings. The image analysis software used with SEM is capable of measuring a grain's 2-D parameters such as diameter, area, and perimeter with binary black-and-white images that are converted from the secondary SEM images. The values of cross-sectional area, perimeter, diameter, length, and width of grains were measured and output in a spreadsheet. The values were labeled on each grain in both the original digital image and in the binary image for ease of comparison to recognize and eliminate any artifacts. In this analysis, only the values for whole grains were considered; all grain fragments were disregarded. The values for roughness, Riley sphericity, and aspect ratio were then calculated using the following equations:

$$\text{roughness} = \frac{\text{perimeter}}{\text{diameter} \times \pi}$$

$$\text{sphericity} = \sqrt{\frac{D_i}{D_c}}$$

$$\text{aspect ratio} = \frac{\text{length}}{\text{width}}$$

where D_i is the diameter of the largest inscribed circle and D_c is the diameter of the smallest circumscribing circle.

3) Direct Shear Test: The angularity of sand grains has been shown to affect the friction angle of sand specimens such that the more angular the grains, the greater the friction angle [38]. The direct shear test is used to determine the friction angle of grains when sheared across a predetermined plane in a shear box. Test specimens collected from the shore-normal transect in February 2007 were prepared in accordance with the American Society

for Testing and Materials standards (ASTM D-3080). Sand samples were oven dried and then rehydrated to a consistent moisture content and relative density. Each sample was then placed in a split-ring shear box apparatus for testing. A normal stress is applied to consolidate the sand before shearing. Upon completion of the consolidation phase, a motorized gearbox drives the two halves of the shear box apart creating a forced shear plane in the sample. Shear stress is measured with a load cell and horizontal and vertical deformation is measured with linear variable displacement transducers. During shear, the normal stress is held constant and a motorized gearbox shears the sand sample slow enough that the sample is allowed to drain and no excess pore pressures are generated. Tests were performed with vertical confining (normal) stresses of 0, 34.5, 69, and 138 kPa. Maximum shear stress for each stage of applied normal stress was plotted as a function of each applied normal stress, and a best-fit regression line through the data points was calculated, from which the friction angle was determined as the arctangent of the slope of the regression.

E. Lignin–Phenol Analysis

Lignin–phenol analyses were performed on the mud fraction of two grab samples (M and F) from the VISSER site, the mud fraction from one diver-collected core from the SAX04 site (FWB17–1), and four grab samples from Choctawhatchee Bay (CBay 1–4). This method has commonly been used to identify terrestrial source materials in coastal sediments [39]–[42]. Lignin is a refractory phenolic macromolecule uniquely found in the structural components of vascular plants [43]. Oxidation of lignin with CuO yields eight dominant vanillyl, syringyl, and cinnamyl phenols, which can be used to distinguish between woody and nonwoody tissues of gymnosperm and angiosperm origin (e.g., seagrasses, mangroves, terrestrial grasses, agricultural plants, and trees) [39], [41], [44].

Freeze-dried sediment samples were analyzed for lignin–phenols using the CuO method of [39], as modified by [40]. Lyophilized sediment samples were weighed to include 3–5 mg of organic carbon and transferred to stainless steel reaction vessels. Samples were digested with CuO in 2N NaOH and in the absence of O_2 at 150 °C for 3 h. Reaction products were extracted with diethyl ether, dried, and converted to trimethylsilyl derivatives with trimethylsilane (TMS) using Bis-(trimethylsilyl)-trifluoroacetamide (BSTFA). Lignin oxidation products were analyzed with an Agilent Technologies, Inc. (Santa Clara, CA) 6890N/5973 gas chromatograph coupled with a quadrupole mass spectrometer (GC-MS). Quantification was based upon internal standards ethyl vanillin and new response factors where generated with each batch by using a mixed standard of the target compounds. While replicates were not performed for each sample, the standard deviation based upon two samples using replicates $(n = 2)$, for the sum of lignin–phenols was less than 8% while that for individual compounds ranged from 1% to 19%.

Lambda-8 (Λ_8) is defined as the sum of vanillyl (vanillin, acetovanillone, vanillic acid) and syringyl (syringaldehyde, acetosyringone, syringic acid) phenols, and cinnamyl (*p*-coumaric and ferulic acid) phenols. Total cinnamyl/vanillyl and syringyl/vanillyl phenols represent C/V and S/V ratios, respectively. Ratios of vanillic acid to vanillin (Ad/Al)v, syringic acid to syringaldehyde (Ad/Al)s were used as indices of lignin decay [44].

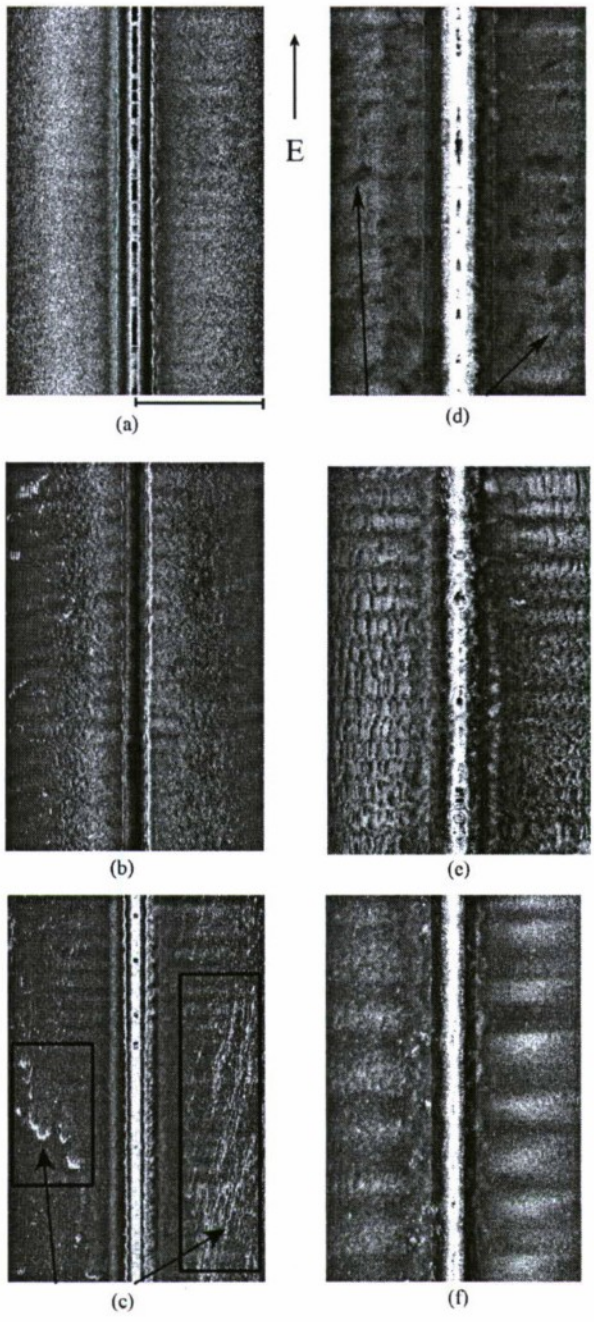

Fig. 2. Sidescan sonar waterfall imagery that provides visual examples of bottom type. Each image has 50-m range and general eastward orientation to the top. Each image is approximately 200 m in length. Lighter shades are higher backscatter. Prestorm images (a)–(c) display small-scale ripple morphology, sinuous mega-ripples, and hardbottoms, respectively. Image (a) displays high backscatter throughout indicative of the small-scale ripple crests found in the prestorm imagery and hardbottoms (c) indicated by the arrows and inside the boxed areas. Poststorm images (d)–(f) show a change in sediment distribution with localized mud-filled depressions, degraded mega-ripples, and lack of hardbottoms. Arrows (d) point to low-backscatter mud-filled depressions. Poststorm images were collected in the same location as prestorm images.

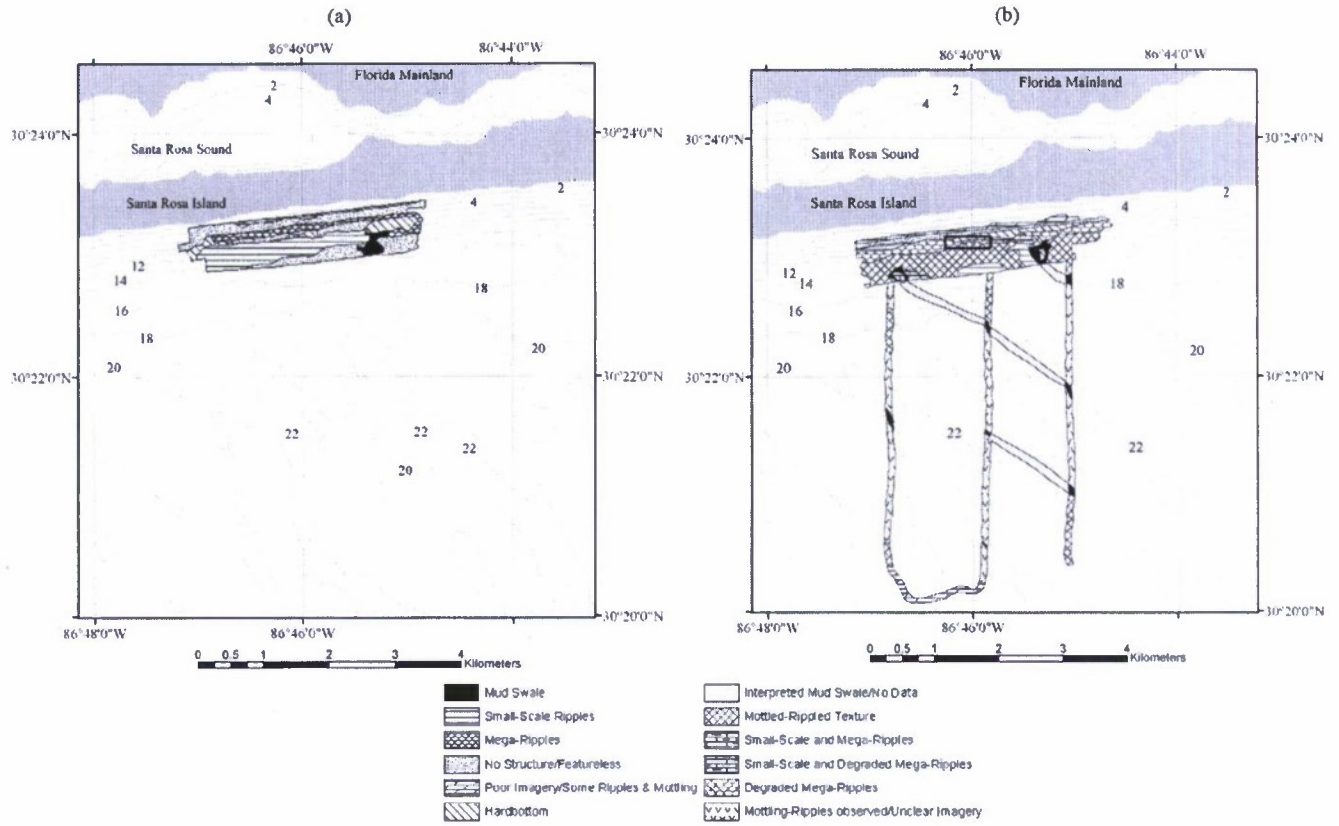

Fig. 3. (a) Pre-Ivan sediment texture map of VISSER site based on sidescan sonar imagery. (b) Post-Ivan sediment texture map based on sidescan sonar and sediment samples. Rectangular box in poststorm map indicates area of multibeam data. Sidescan sonar waterfall images presented in Fig. 2 are morphologic examples used to construct these textural maps.

IV. Results

A. Acoustic Imagery

Sidescan sonar imagery revealed several morphologic and textural changes to the seafloor following Hurricane Ivan that provide a glimpse into sediment distribution patterns following a major storm event (Fig. 2). Sediment morphologic and characteristic boundary maps were constructed based on sidescan sonar imagery both before and after Hurricane Ivan (Fig. 3).

Sonar imagery collected before Ivan's landfall reveals four general bottom characteristics. First, the study area is mostly a sand bottom with regions of uniform, small-scale wind-wave ripple morphology that exists mostly in water depths greater than 10 m on the western side of the survey area [Fig. 2(a)]. The ripple orientation is shore-normal, with crests and troughs extending in the E–W direction. Spacing between ripple crests is approximately 0.5–0.6 m.

Second, the ripple morphology is less apparent on the eastern side of the survey area where sonograms show a continuous area oriented E–W through the middle of the survey area in about 6 m of water that exhibits a sinuous-mottled texture [Fig. 2(b)]. This indicates possible mega-ripples. The rippled morphology disappeared in the shallow areas (<4 m) with little or no apparent bottom structure.

Third, scattered areas of high backscatter appeared that stretched discontinuously through the middle of the survey in about 9 or 10 m of water 0.5 km offshore, in slightly deeper water than the detected mega-ripples. Similar features also appeared in a small area close to the shore directly in front of the VISSER tower. These high-backscatter features often exhibited a thin, linear, NE–SW directional trend, but they also appeared in a thick zigzag or cuspate shape of extreme high backscatter in some locations. These areas are interpreted to be hardbottoms. Hardbottoms are common along the MAFLA sand sheet and the inner continental shelf of the northeastern Gulf [45], [46]. The hardbottoms are the exposed, resistant Pleistocene deposits partly veneered by the thin sand sheet that was mobilized during the Late Pleistocene and Holocene eustatic sea-level rise and reworked during modern times.

The fourth, and most prominent seafloor feature of the pre-hurricane sonar imagery, is a distinct area of low backscatter at the eastern end of the survey area in water depths greater than 10 m. This area is interpreted to be a mud swale. Although the shelf slope decreases between water depths of 9 and 18 m, the 18-m contour curves toward shore, approaching the area where the mud swale was detected.

Following Hurricane Ivan, this mud swale on the eastern end of the survey area narrowed spatially, as defined by the areal extent of low backscatter, yet the boundary of the swale became less diffuse (Fig. 3). The swale trends in a NW–SE direction much like the subtle bathymetric trend in the immediate area, and is clearly shown in the posthurricane sonar imagery (Fig. 4). An additional mud swale became evident, albeit less distinct, on the western end of the survey area in the post-Ivan imagery.

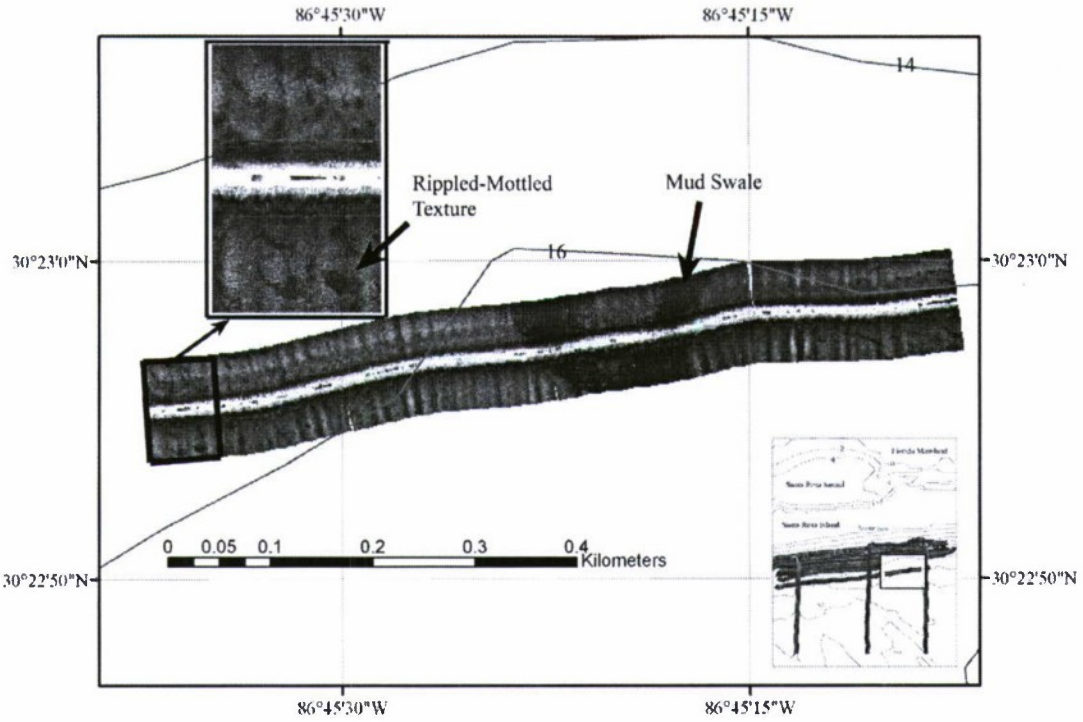

Fig. 4. Poststorm sidescan image of mud swale surrounded by areas exhibiting the ripple-mottled texture of small-scale ripples and mud-filled depressions. The location of this image is noted by the box in the vicinity map in the lower right corner of the figure. Two bathymetric contours (14 and 16 m) indicate depth of the area. The western edge of the image is enlarged to show the mottled texture of mud-filled depressions and small-scale ripple morphology. This texture is also visible east of the mud swale.

Furthermore, mud swales were detected farther offshore from the primary survey area. These mud swales, revealed after the storm by the three shore-perpendicular survey tracks that extended into deeper water, also trend NW–SE and occur for at least 5 km offshore into 21-m water depth. The mud swales detected in each shore-perpendicular transect are inferred to be continuous with the near-shore mud swales in the primary survey area, although the nearly 1.5-km separations among the survey tracks exclude the definitive evidence of the mud swales' shoreward continuity. Based on their concordant angle and trend to shore, the offshore mud swales are likely continuous with the mud swales detected in the near-shore, shore-parallel transects. The mud swales generally follow the bathymetric lows of the ridge-and-swale topography of the region.

The most obvious morphology change in the poststorm imagery, however, was the mottled texture created by high-backscatter sand ripples amid low-backscatter patches [Fig. 2(d)]. The area of a typical low-backscatter patch was 25 m^2, but the patches varied in size and shape. Diver observations just 5 km to the east confirmed the existence of mud deposits, or mud-filled depressions. Observations on the thickness of the mud ranged from thin, 2-cm layers up to 15-cm mud deposits concealing all but the largest amplitude sand ripple fields. This mottled texture dominates most of the seafloor sonar imagery in the deeper water. However, some smaller areas exhibit solely the ripple morphology without the mud deposits. Posthurricane sonar imagery shows larger crest-to-crest spacings (approximately 0.6–0.7 m) between ripples than the prehurricane imagery. Another poststorm change in the seafloor features was that the mega-ripples apparent in the center of the prestorm imagery now appear degraded. Greater amounts of mud were deposited in the troughs creating greater backscatter contrast from the ripple crests.

The hardbottoms that stretched through the featureless sand and mega-ripples before Hurricane Ivan largely disappeared after the storm. Poststorm sonar imagery shows some scattered areas of hardbottoms in the same water depth, but the area narrowed spatially in the offshore direction and became less prominent in the sonar imagery. A directional trend is not apparent as in the prestorm imagery. Nevertheless, hardbottoms sporadically appear in the same water depth from the eastern to western edge of the survey area [Fig. 3(b)], and could be considered more extensive in the along-shore direction. But this middepth region of the study area exhibited a more varied mix of small-scale and degraded mega-ripples, hardbottoms, and featureless sand following Ivan. Troughs of the mega-ripples appear to have collected fine-grained material following the storm.

The multibeam backscatter imagery (Fig. 5) provides a much better overall picture of the poststorm seafloor morphology in the center of the survey area that is hard to interpret with sidescan sonar imagery. The multibeam imagery makes apparent the sinuous pattern of the degraded mega-ripples with acoustically reflective sand ripples that finger-out into the less acoustically reflective areas that indicate little relief. Kraft and de Moustier [35] present additional multibeam data in this issue that provide evidence of poststorm sediment transport from the barrier island to the offshore. Sediment accumulation was highest in the shallow area of the tower survey site decreasing in the offshore direction with net erosion in the deepest areas.

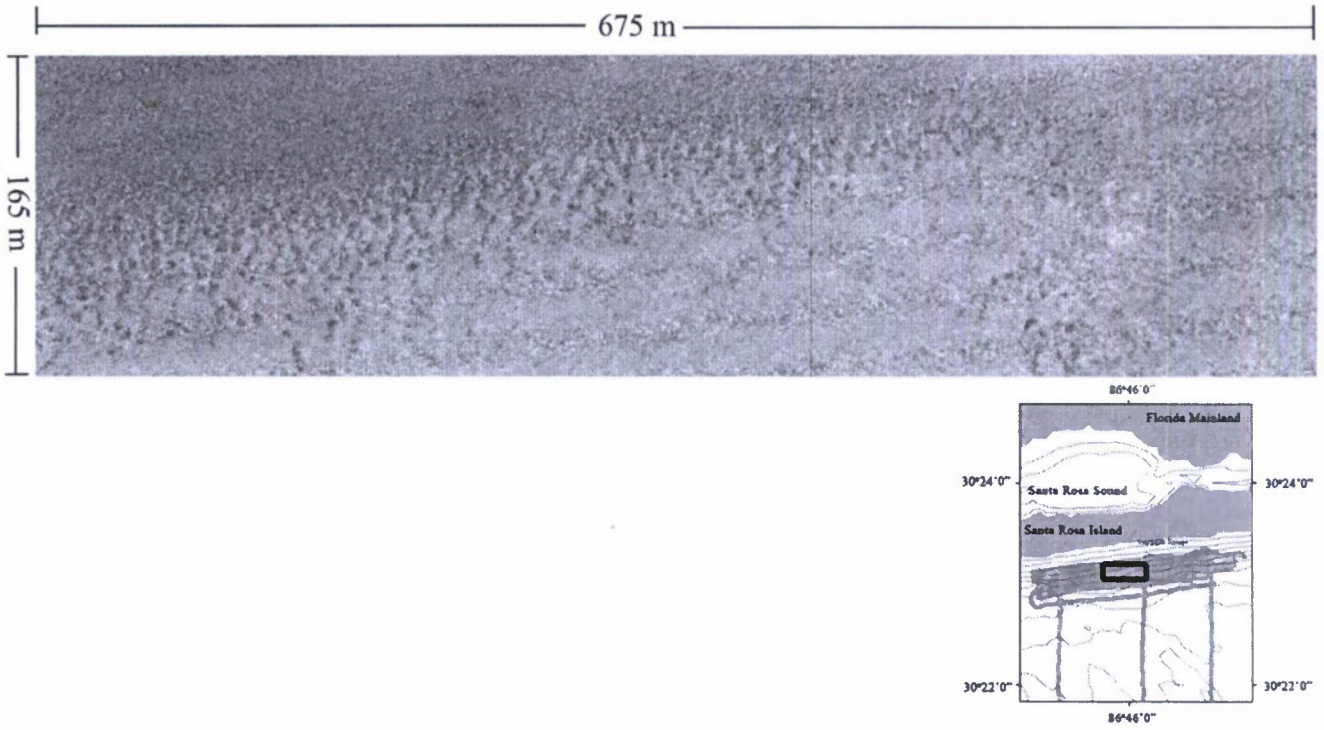

Fig. 5. Multibeam data collected October 27, 2004, 41 days after Hurricane Ivan passed over the area. Backscatter data collected with EM3002 draped over Reson 8125 bathymetry (25-cm grid). (Modified from [35].)

B. Sediment Characterization

1) Grab Samples: The surficial sediment throughout most of the study, as determined from the grab samples, is fine to medium sand and moderately sorted or moderately well sorted (Table I), similar to the sediments at the SAX04 site as described in [47]. The deeper region, consisting of mostly rippled sand or rippled sand with mud-filled depressions, is moderately sorted or moderately well-sorted medium sand. The shallow areas are typically fine sand (very near medium sand), and well sorted. The sediment in the shallow area is sugary white fine to medium sand indistinguishable from the subaerial beach and dune sand of the barrier islands of the Florida panhandle. The sediment in the middepth area, which exhibits small-scale and degraded mega-ripple morphology in the sonar imagery, is texturally similar to the other samples. Yet, these samples contained slightly elevated mud contents of 1.7%–2.8% (by weight) consisting mostly of clay-sized particles, whereas most samples from the study area contained even less mud of predominantly silt. One grab, located near the edge of the eastern mud swale, contained the highest mud content at 2.8% and more than 5% gravel-sized shell fragments, as opposed to most samples with negligible amounts of shell fragments.

All but four of the 15 grab samples collected in the offshore transect are considered medium and moderately well-sorted sand. Two sites nearest the beach, N and O, are fine sand (nearly medium sand). They are also better sorted and quite similar to the 11 beach samples collected to the base of the VISSER tower. Grabs M and F each contained mud in the form of a flaser deposit, described as ripple bedding in which the deposition of suspended fine-grained mud drapes the rippled sandy seafloor during quiescent periods followed by the migration of sand ripples due to strong currents [47] (Fig. 6). Grab F was collected very close to one of the offshore mud swales, and within the area of mud-filled depressions. The location of this sample was in water at least 2 m deeper than adjacent grabs G and E. A mud swale is not evident in the sonar imagery at the location of grab M, but it was sampled from a region characterized by sand ripples and the patchy mud deposits where the barrier shoreface slope decreases. Subsequent to burial by sand ripple migration, the mud sequestered in flasers would not be detected in the high-frequency sonar survey of the area.

The mud flasers in grabs M and F are silty clay deposits. The sand fractions, with greater amounts of fines than other sand samples, are very fine and fine sand, respectively. However, the sand fraction of grab M contained nearly 22% mud (silt + clay) compared to 3% in grab F. Therefore, the sand fraction in grab M is very poorly sorted muddy sand collected at the base of the barrier shoreface, as opposed to grab F that is moderately sorted fine sand located 3.5 km offshore near a bathymetric low or mud swale.

The mud flaser deposits are texturally similar to the Choctawhatchee Bay samples (Table I). CBay2 and CBay3 have a mean grain size almost identical to the mud flaser deposits in grabs M and F. CBay4, collected near the mouth of the Bay, is the coarsest sample from Choctawhatchee Bay, but is composed of mostly (71%) clay, as are the other bay samples and the flasers in offshore sediment.

a) Origin of Mud: Various compositional analyses were performed on the mud fraction to establish its provenance (Table II). The severe erosion of the beach dune complex and aerial images of turbid discharge from the bay following the

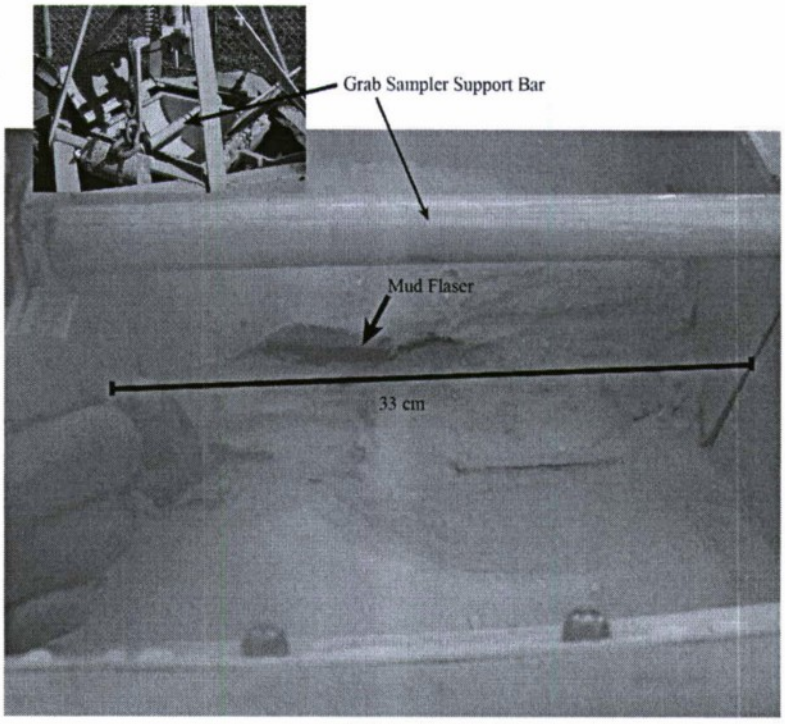

Fig. 6. Mud flaser deposit (arrow) inside Smith–McIntyre grab sample bucket. Mud is ~2 cm thick draped by ~3 cm of medium-sized sand. Bucket width is approximately 33 cm indicated by black line.

hurricane are anecdotal evidence of an outwash and deposition of lagoonal mud following the inundation of the barrier island, breaching of the barrier dunes, invasion of the lagoon, and retreat of the storm surge. Initially, only $\delta^{13}C$ isotope and organic carbon and nitrogen composition measurements were assayed from flasers and lagoon sediment to characterize the source of the organic matter within the mud. The isotopic carbon fractions of the three offshore sites (two along the shore-normal transect and one [FWB17-1] from the SAX04 site) are similar to the inshore sediment sample at VISSER (Table II). However, the location of the VISSER lagoon sample immediately behind the overwashed barrier island and the relative coarseness of the sediment sample (98.5% medium sand) means that the sediment is probably contaminated with dune sand, or even shelf sand. In fact, there is scarce organic carbon present in the sample. Lacking conclusive evidence of the source of the offshore mud deposits, various radionuclides were assayed in new samples from within Choctawhatchee Bay as well as some of the offshore samples from 2004 (Fig. 1). The ^{7}Be radionuclide data are not directly useful because the isotope's relatively short half life (53 d) resulted in the isotope being undetectable 28 months after the samples were collected in 2004. Of those lagoon samples containing measurable concentrations of ^{7}Be (CBay3 and CBay4), CBay3 contains elevated concentrations indicating deposition within one year. The CBay3 sample also contained the highest concentration of ^{137}Cs in all of the lagoon samples. The elevated concentration of ^{7}Be and ^{137}Cs in CBay3 may indicate the most recent surficial deposition and the least erosive setting. The wide range of excess ^{210}Pb concentrations indicates variable stability among stations. The offshore mud contained the highest excess ^{210}Pb concentrations, which may indicate a different source, or be an indication of contrasts in organic matter content or reduced sediment mixing. Elemental analyses (organic carbon and nitrogen) show similarities between lagoonal and offshore mud, with mud from both locations exhibiting a C:N ratio around 9. Despite these data, determination of the provenance of the offshore mud deposits is not conclusive without a biochemical fingerprint-type analysis of the organic matter associated with the mud.

Lignin–phenol analysis provides a more conclusive indication of the origin of the offshore mud deposition. Lignin–phenol concentrations (Λ_8) ranged from 0.45 to 1.28 across all stations, with the highest and lowest values at CBay4 and FWB17–1, respectively (Table II). There was a gradient of decreasing Λ_8 moving from the inlet (CBay4) to the inner bay stations. The lowest Λ_8 value was found at the deepest sediment layer (7–9 cm) from core FWB17–1 collected on the shelf. Conversely, the (Ad/Al)v ratio at the FWB17–1 deep layer was less degraded than the upper 0–7 cm at the FWB17–1 station. The S/V and C/V ratios indicated that the primary lignin source was nonwoody angiosperms. The highest S/V and C/V ratios were found at CBay1 in the inner bay and the FWB17–1 station, respectively.

Based on our lignin analyses, the mud sediments found on the inner Florida shelf appear to have been derived from inner bay or estuarine sources and freshly deposited following Hurricane Ivan. The gradient of decreasing Λ_8 could be interpreted as transport of material from the shelf into the bay, or a removal of stored material in the inner bay stations to the inlet, where the highest Λ_8 occurred. Since the inner shelf in this region is not typically composed of fine-grained mud commonly

TABLE I
MEAN GRAIN SIZE (M_z), SORTING COEFFICIENT (σ) IN PHI UNITS, AND PERCENTAGES OF GRAVEL, SAND, SILT, AND CLAY FOR SEDIMENT SAMPLES IN THE STUDY AREA. SEE FIG. 1 FOR LOCATIONS

Station	M_z	σ	% Grav	% Sand	% Silt	% Clay
A	1.44	0.69	0.27	98.27	0.18	1.27
B	1.73	0.53	0.00	98.28	0.63	1.09
C	1.64	0.60	0.03	98.89	0.09	0.99
D	1.63	0.66	0.08	98.30	0.55	1.06
E	1.68	0.50	0.00	98.75	0.22	1.04
F1†	10.27	2.79	0.00	0.60	25.86	73.53
F2	2.13	0.73	0.02	96.93	1.52	1.53
G	1.62	0.61	0.07	97.79	0.88	1.26
H	1.34	0.63	0.10	98.40	0.72	0.77
I	1.26	0.64	0.10	98.18	0.59	1.13
J	1.04	0.71	1.12	97.06	0.50	1.32
K	1.56	0.66	0.00	97.94	0.19	1.88
L	1.54	0.60	0.00	98.14	0.58	1.28
M1†	10.63	2.59	0.00	3.73	15.10	81.17
M2	3.30	3.51	0.23	78.02	6.58	15.17
N	2.23	0.43	0.01	98.74	0.23	1.01
O	2.06	0.64	0.01	98.26	0.60	1.13
1	2.09	0.61	0.05	97.97	0.75	1.23
2	1.65	0.78	0.00	97.64	1.13	1.24
3	1.82	0.73	0.00	97.21	1.57	1.22
4	1.88	0.66	0.29	98.01	0.19	1.51
5	1.36	0.74	0.12	98.50	0.16	1.23
6	2.19	1.17	5.22	91.99	0.98	1.81
7	2.26	0.46	2.56	95.57	0.55	1.33
8	2.11	0.50	0.16	99.09	0.25	0.49
9	1.49	0.71	0.09	98.35	0.83	0.73
10	1.76	0.71	0.15	98.68	0.42	0.75
11	1.80	0.61	0.02	98.52	0.64	0.82
12	2.09	0.45	0.01	98.16	1.05	0.78
13	1.95	0.70	0.00	97.66	1.30	1.04
14	0.96	0.67	0.07	98.76	0.20	0.97
15	2.07	0.57	0.91	97.47	0.40	1.22
VISSER	1.63	0.47	0.00	98.46	0.28	1.26
CB1	11.12	2.44	0.41	3.35	10.50	85.74
CB2	10.68	2.06	0.00	0.85	11.61	87.54
CB3	10.37	2.46	0.00	3.34	14.07	82.58
CB4	9.36	3.17	0.00	13.10	16.00	70.90
FWB17-1*	11.27	2.56	0.00	1.48	14.92	83.60

†flaser deposit
*5-7 cm interval only

found farther west and the composition of lignin is different from western deltaic sources, the mud and associated terrestrial organic carbon is likely from the back-barrier bays of the region. The Λ_8 gradient within the bay, and the similarity to the mud collected offshore in sample M, supports accumulation of estuarine mud offshore. In addition, the mud layer in SAX04 core FWB17–1 does not follow the ordinary diagenetic profile of lignin, but instead resembles the profiles found on the Louisiana shelf that show mobilization of large amounts of sediments, organic carbon, and deposition of storm layers with a net direction from land-to-sea off the Mississippi River delta for Hurricanes Ivan, Katrina, and Rita [48], [49]. This further indicates that the mud was recently deposited on the shelf following outflow from the back-barrier bays.

The lignin sources of sediments on the Florida shelf were not derived from the redistribution of mud sediments from the Mississippi River delta. The C/V and S/V ratios indicate a non-woody source of lignin, similar to the Louisiana shelf, but the S/V ratios were slightly lower and the C/V ratios higher. This may indicate local sea grass inputs. Lignin biomarkers have been used extensively along the Louisiana coast, specifically within the Mississippi River [42], [50], on the Louisiana shelf [51], [52], and in the Mississippi Canyon [52], and the lignin

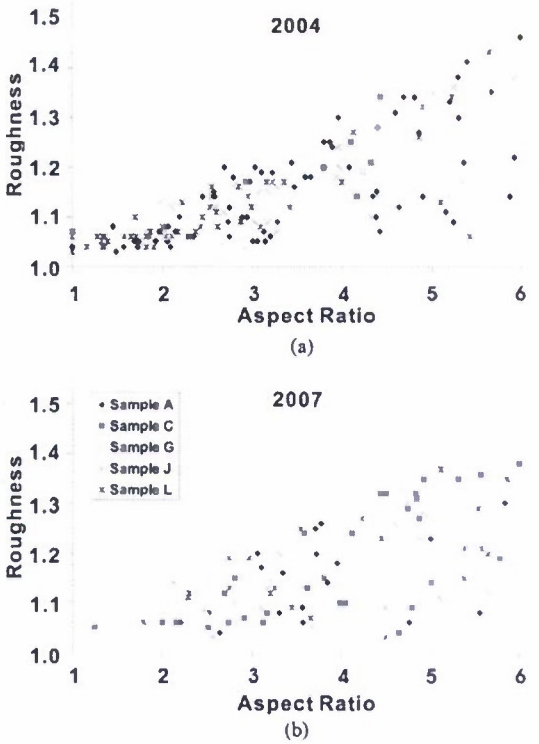

Fig. 7. Plot of grain roughness as a function of grain aspect ratio for five grab samples (A, C, G, J, and L) collected in (a) 2004 and (b) 2007.

sources are clearly significantly different than those observed here. We cannot explain the difference in the ratios between grabs F and M, separated by 2.5 km in the offshore direction, but perhaps different sea grass input over this distance is further indication of offshore mud transport from the back-barrier lagoons rather than simple redistribution of mud previously deposited on the shelf.

b) Particle Characterization: Average grain shape of the sand at the Santa Rosa Island study site was generally more elongate, platy, and bladed than compact (Table III). Riley sphericity showed little change (0.82–0.85) along the shore-normal transect immediately after Hurricane Ivan. However, the aspect ratio increased slightly at the deeper offshore sites (from about 2.29 to 3.38). The roughness of the grains increased from about 1.10 ($\pm$0.11) for the location closest to the shoreline to about 1.34 ($\pm$0.22) for the farthest offshore location. There are significant differences ($\alpha < 0.05$) in sphericity and roughness values between inshore and offshore locations (L versus A or VISSER tower versus A).

Sediment from the same shore-normal transect was newly collected in 2007 to determine any changes in grain shape factors and thus, sediment transport during the three-year interim. The grain size distributions for 2004 and 2007 exhibit some differences (Table III). However, despite nearly identical mean diameter values from the sieve analyses at locations A, C, and J, the 2007 samples are slightly better sorted (have smaller standard deviation values) than the 2004 samples. Riley sphericity values, as in 2004, exhibit little change (0.74–0.79) between offshore (A) and inshore (M) locations. However, the grain sphericity and roughness values at locations A, C, and L

TABLE II
RADIONUCLIDE AND ORGANIC COMPONENTS OF SEDIMENTS FROM OFFSHORE AND BARRIER ISLAND LAGOON (INCLUDING CHOCTAWHATCHEE BAY [CBAY]) MUD SAMPLES

Sample ID	date sample collected	avg $\delta^{13}C$ TOC	stdev $\delta^{13}C$ TOC	avg amt% TOC	stdev amt% TOC	^{7}Be (mBq/g)	^{137}Cs (mBq/g)	$^{210}Pb_{xs}$ (mBq/g)	%C	%N	C:N	A8	A6	(Ad/Al)v	(Ad/Al)s	C/V	S/V
Offshore																	
M(mud)	Sep-04	-19.65	0.04	5.1	0.08	0**	3.14 ± 0.34	408.23 ± 14.10	4.51 ± 0.07	0.49*	9.23	0.80	0.61	0.56	0.30	0.44	0.46
F(mud)	Sep-04	—	—	—	—	0**	2.03 ± 0.22	364.85 ± 12.24	4.64 ± 0.09	0.55 ± 0.09	8.49	0.56	0.38	0.50	0.29	0.64	0.39
FWB17-1 (1-3cm)	Oct-04	-19.76	0.15	4.26	0.15	0†	—	—	—	—	—	0.84	0.55	0.66	0.39	0.77	0.46
FWB17-1 (5-7cm)	Oct-04	—	—	—	—	—	—	—	—	—	—	1.07	0.77	0.57	0.38	0.57	0.47
FWB17-1 (7-9cm)	Oct-04	—	—	—	—	—	—	—	—	—	—	0.45	0.36	0.37	0.28	0.38	0.44
Lagoon																	
VISSER	Aug-05	-20.52	0.63	0.1	0.02	—	—	—	—	—	—	—	—	—	—	—	—
CBay1	Jan-07	—	—	—	—	0**	2.29 ± 0.23	72.57 ± 2.63	2.51 ± 0.16	0.26 ± 0.01	9.68	0.69	0.58	1.03	0.54	0.36	0.86
CBay2	Jan-07	—	—	—	—	0**	4.74 ± 0.46	219.32 ± 7.55	3.77 ± 0.26	0.42 ± 0.01	8.99	0.95	0.76	0.56	0.28	0.43	0.68
CBay3	Jan-07	—	—	—	—	12.37 ± 0.92	15.94 ± 1.52	197.51 ± 6.25	3.48 ± 0.02	0.40*	8.72	1.06	0.84	0.45	0.27	0.42	0.67
CBay4	Jan-07	—	—	—	—	4.94 ± 0.32	3.41 ± 0.34	186.82 ± 6.13	3.18 ± 0.13	0.36 ± 0.01	8.81	1.28	1.03	0.60	0.28	0.39	0.58

*standard deviation < 0.01, ** value below the detection limit, † Sep 2004 sample by R. Wheatcroft.

TABLE III
AVERAGE VALUES OF GRAIN SHAPE PARAMETERS FOR SANTA ROSA ISLAND SITE AND SAX04. DIAMETER[1] IS DETERMINED FROM SEM IMAGE ANALYSIS; DIAMETER[2] IS DETERMINED FROM SIEVE ANALYSIS; VT IS LOCATED AT THE VISSER TOWER; SAX04 SAMPLES ARE FROM CORE FWB20-1

	Santa Rosa Island 2004						Santa Rosa Island 2007						SAX04 (2004)	
	A	C	G	J	L	VT	A	C	G	J	L	M	0-2cm	22-24cm
Diameter[1] (mm)	0.47	0.51	0.59	0.50	0.65	0.24	0.42	0.27	0.34	0.45	0.41	0.36	0.66	0.77
Diameter[2] (mm)	0.37	0.32	0.32	0.49	0.34	0.38	0.38	0.32	0.40	0.49	0.43	0.44	0.37	0.40
Aspect Ratio	3.01	3.38	3.12	3.11	2.29	3.15	4.76	4.79	4.09	3.82	3.37	4.05	2.97	2.95
Sphericity	0.81	0.85	0.80	0.82	0.83	0.74	0.75	0.76	0.77	0.76	0.79	0.74	0.82	0.81
Roughness	1.34	1.18	1.17	1.14	1.10	1.08	1.20	1.22	1.16	1.14	1.13	1.11	1.14	1.14
Friction Angle (°)	—	—	—	—	—	—	47.6	47.3	45.9	45.7	44.5	44.2	—	—

are significantly different ($\alpha < 0.05$) in 2007 when compared to the same locations in 2004. Also, the values of grain aspect ratio change, with grains appearing more elongate in 2007 than in 2004. The grain shape distribution of sand samples collected in 2004 and 2007 exhibited a slightly different distribution of roughness as a function of aspect ratio (Fig. 7). The grain shape distribution in 2004 has a larger cluster of low-roughness/small-aspect-ratio particles than the distribution measured at the same locations in 2007. The sand off Santa Rosa Island in 2007 is lacking in the less rough, more spherical grains that were more numerous on the surface immediately following the passage of Hurricane Ivan in 2004. The scatter plot in Fig. 7 indicates a general trend in the similarity between the aspect ratio and the roughness of the grains. This positive trend indicates that platy and elongate grains tend to have more roughness elements than rounded and compact grains. This observation could merely be the natural effect on grains of mechanical weathering and abrasion over time.

Values of shape parameters for the surface and 25-cm-deep sands from the core from SAX04 are very similar to the values for the surface sands from the Santa Rosa Island study site, which were collected at the same time (2004). The average grain size obtained from the SEM images is biased towards slightly coarser values than the mean nominal diameter as determined from sieve analysis (Table III), especially for the 2004 samples. This is to be expected, as sieve analysis operationally defines the minimum diameter as the nominal diameter by allowing the smallest dimension to pass through the mesh.

The values of the friction angle were determined for samples collected at sites A, C, G, J, L, and M in 2007. Friction angle of the grains increased from 44.2° at the site closest to shore (M) to 47.6° at the site farthest offshore (A) along the VISSER transect. Although there was not much variation in value of friction angle among samples collected along the transect, there is a trend of increasing grain angularity (as indicated by friction angle or grain roughness) with increasing depth and distance from shore.

2) Vibracore Samples: The vibracores collected at the VISSER and SAX04 sites provide insight into the lithology of the upper 5 m of subsurface, and provide useful geologic perspective to sediment distribution. At least three of the six sedimentary facies historically identified between Pensacola and Mobile Bays [18], [19] were identified in this study. Results from two example vibracores are provided (Figs. 8 and 9). Vibracore 1C was collected at the SAX04 site in 15.5 m of water, but is analogous to cores collected at the VISSER site (e.g., Vibracore 25).

Generally, the upper 3 m (but as much as 4.5 m) of substrate comprised mostly gray to tan medium shelly quartz sand with various amounts of shell hash (Fig. 8). Sporadic large shell frag-

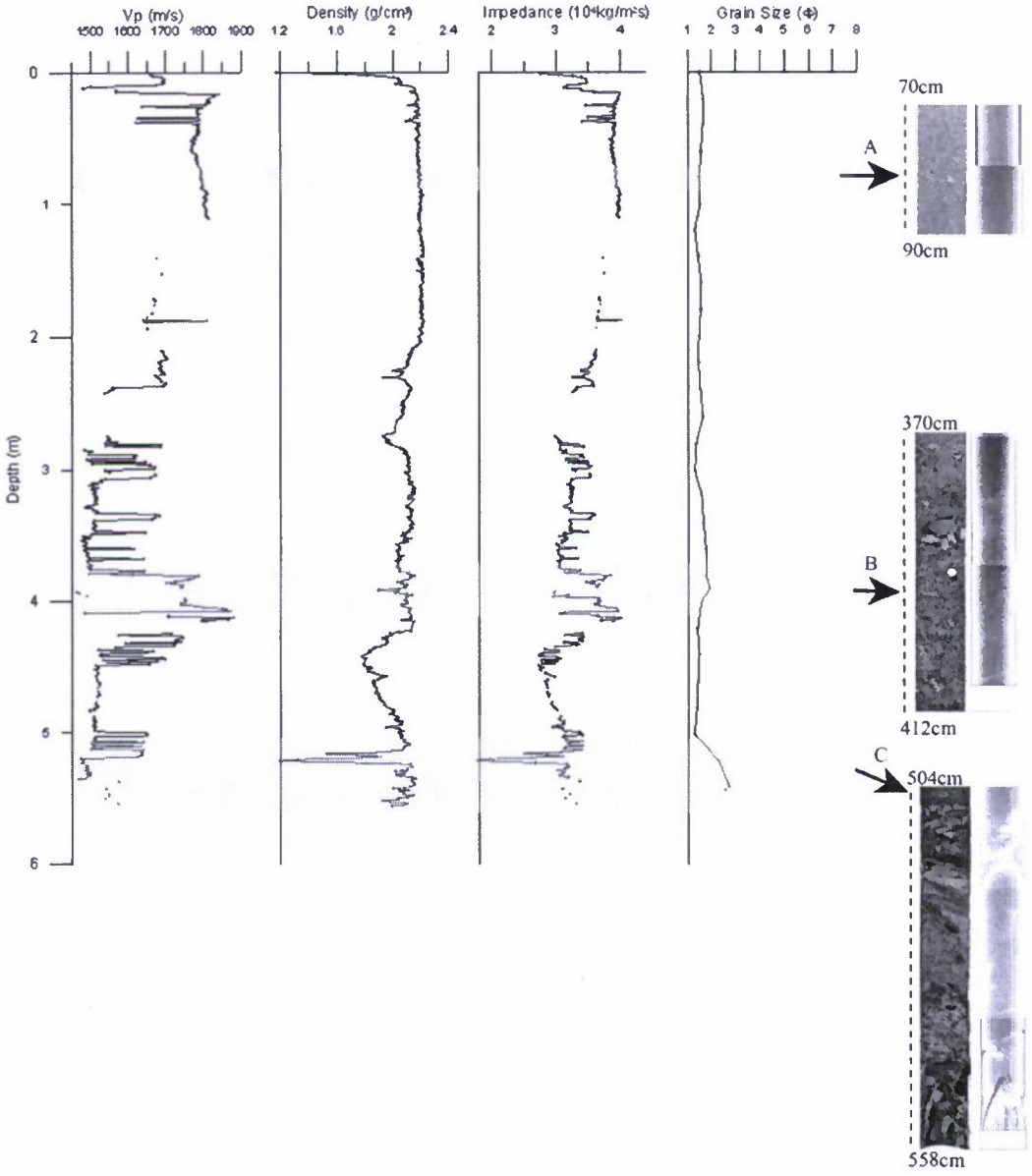

Fig. 8. Multisensor core logger and grain size data from vibracore 1C at the SAX04 site, with selected core photographs (left) and X-radiographs (right) that correspond to the plots with transparent bars. Dashes along core sections are 1-cm intervals, and the depth of the top and bottom of each core section are identified. P-wave speed (Vp) and impedance plots are discontinuous due to poor data as a result of the use of aluminum liners and scattering of acoustic signal from shells and shell fragments. Image A is medium sand corresponding to Facies 6. Image B shows the matrix-supported shell layer of Facies 5, although somewhat minimal in this example. Deeper than 4 m bsf is Facies 4 with greater mix of fine material, wood, peat, and sand as shown in image C. The X-radiograph in image C shows density variability due to this layering.

ments and whole shells (typically sand dollar or mollusk shells), or a thin shelly layer occasionally appeared in the upper 3 m. Density values for this unit are 2.0–2.2 g/cm^3, which are typical for unconsolidated shelf sands. Sediment P-wave speed values usually varied between 1740 and 1810 m/s. This unit is largely homogeneous, clean, medium sand corresponding to Facies 6 described in [20]. A matrix-supported shell bed appeared at the base of Facies 6 (Figs. 8 and 10) often with whole mollusk or echinoderm shells, with many of these shells appearing pristine. The shell bed is at most 0.5 m thick and corresponds to Facies 5. Unfortunately, this shell bed often prevented deeper core penetration. Overall, the upper 3 m of substrate is a thick deposit of rather homogeneous, moderately or moderately well-sorted, medium sand representative of the MAFLA sand sheet, but truncated by a shell bed containing large bioclasts.

Greater variability and more sedimentary structure exist below the shell bed, generally deeper than 3 m below the surface (bsf). Mud, shell, and peat layers intermix with the medium sand, thus forming distinct layers, simply changing the total composition, or providing various mottling appearances. Sedimentary structure is more complex as exhibited in X-radiographs (Figs. 8 and 9). The sand in this underlying unit is often brown in color as opposed to the clean gray or tan sand of Facies 6. But fine-grained beach-like sand does appear at various spots throughout the cores. The amount of fine-grained material increases from 1%–2% in Facies 6 to 3%–20% in the

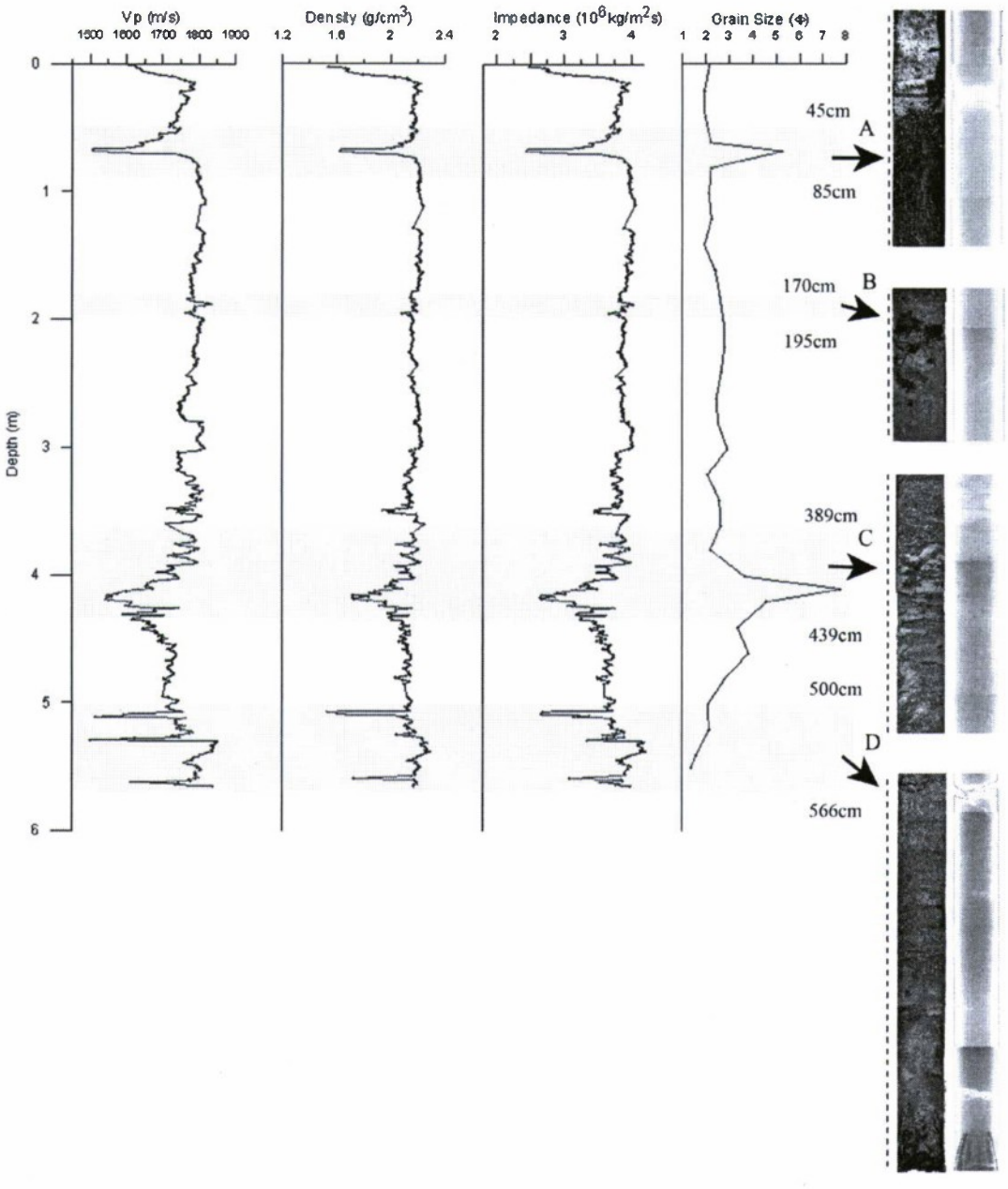

Fig. 9. Multisensor core logger and grain size data from vibracore 25 along the east flank of the VISSER site, with selected core photographs (left) and X-radiographs (right) that correspond to the plots with transparent bars. Dashes along core sections are at 1-cm intervals, and the depth of the top and bottom of each core section are identified. Image A contains clayey layer present at about 0.65 m bsf separating the Facies 6 sand unit above an organic-rich fine sand. This corresponds to Facies 4 much shallower than in vibracore 1C. Peat and wood appear in image B at 2 m in fine sand (sand is orange brown in color). Multiple clayey and mud layers appear 3.5–4.5 m bsf in image C. Consolidated tan muddy sand exists below 5-m depth in image C. Burnt orange sand also appears and may indicate rip-up clasts and transition into Facies 3.

underlying unit. Highly organic layers, including vegetation (peat, wood, and conifer cones), appear regularly to the greatest depths attained in cores (5.6 m bsf). This unit likely corresponds to Facies 3 and/or 4 in [18].

However, the upper 3 m of subsurface is not composed entirely of a clean (mud-free), shelly, medium quartz sand, as shown in the shore-perpendicular vibracore transect (Fig. 11). Vibracores 18 and 20 were collected in bathymetric lows or locations where the shelf slope decreases offshore, and exhibited different characteristics than the other cores. Vibracores 16 and 17 were collected near shore in only 4 and 8 m of water, respectively, and comprised entirely the shelly quartz sand of Facies 5 and 6. Vibracore 17 probably just penetrated into the underlying units at approximately 4.5 m bsf, and provided the thickest example of the Facies 6 sand unit sampled in this study. Yet vibracore 18, collected just 200 m seaward of 17, consisted of dark brown and highly odorous sand high in organic matter beginning less than 8 cm below the sediment surface. The grain texture of the sediment in the upper 3 m of vibracore 18 is perhaps not significantly different than the other cores, classified as a moderately sorted fine sand with 3%–5% mud content, but a 30-cm-thick clayey peat layer containing wood lies just 1.5 m

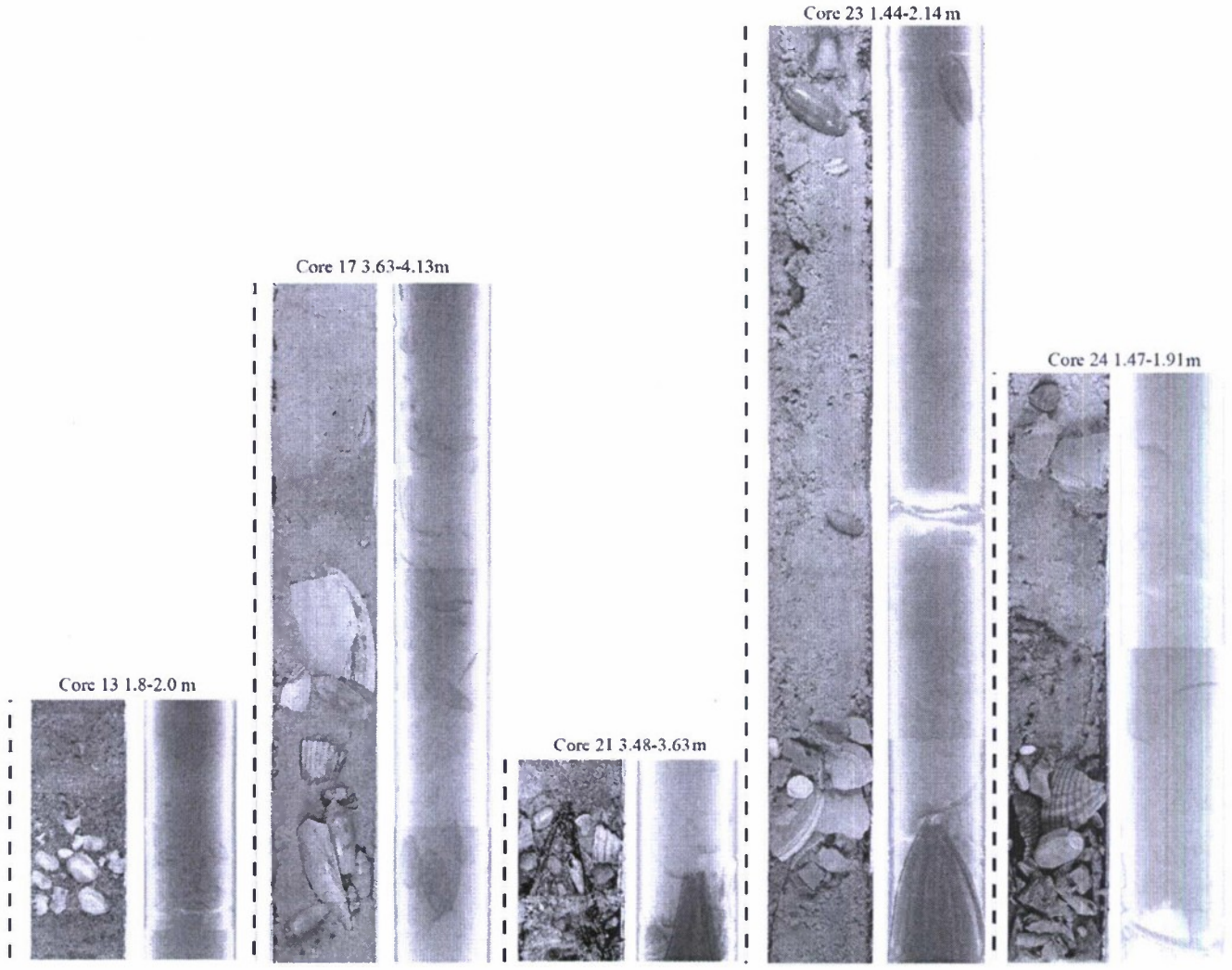

Fig. 10. Example photographs (left image) and X-radiographs (right image) of the shell bed of Facies 5 and its various depths in some of the vibracores. Shell bed composed largely of pristine mollusk shells, and other animal shells. Images not to scale with each other; depths noted next to each image are in meters with a 1-cm dashed scale bar alongside each image.

bsf. Moreover, the sedimentary structure of vibracore 18 becomes more variable deeper than 3 m bsf with 5%–17% mud until the sediment returns to cleaner sand deeper than 5 m bsf. The location of vibracore 18 is nearly colocated with a grab (M) that sampled a clay flaser deposit. Both the thin extent of sediment overlying the organic-rich layer and the presence of ponding of mud that contributes to flaser development at this site might be explained by bathymetry. Vibracore 18 and grab M were collected in a 6-m-deep depression, where the typical shelf swale morphology exposes older strata and offers a low-energy shelter in which fine sediments collect.

The shelf slope again increases seaward toward grab K and vibracore 20. These samples are located on the 18-m isobath as it completes its landward trend and returns seaward. Therefore, they were collected at the edge of a bathymetric low and a mud swale. The upper 70 cm of vibracore 20 comprised the Facies 5 and 6 sand, but Facies 4 appeared 90 cm bsf with muddy peat horizons and dark green or gray organic-rich muddy sand. Thin clayey layers, as in core 18, are present deeper than 2.4 m bsf before returning to a cleaner medium sand around 2.6 m bsf.

Vibracore 25 was collected in the same water depth as vibracore 18, but along the eastern flank of the study area, and contained more strata throughout its length (Fig. 9). A 3-cm-thick, clayey sand layer appeared 67 cm bsf, separating the overlying Facies 6 from a dark, organic-rich, moderately sorted fine sand with an increased amount of fine material below. The dark color is a result of the presence of peat and reduced (sulfide) clay layers. Conversely, in vibracore 21 on the western flank, Facies 6 was found deeper, extending from 3.5 m bsf to the shell bed. The water depth from which vibracore 21 was collected was shallower (9 m) than that of vibracores 18 and 25 due to a gentler shelf slope off the barrier island. Vibracores 18 and 25, located at the base of the barrier-shoreface in a bathymetric low, contained the most variability nearest the surface and the greatest amount of fine-grained material. Maximum core penetration and recovery of over 5.5 m occurred at these two deeper locations. These vibracores likely penetrated into Facies 3, as described in [18], but not likely into the deeper Pleistocene units. There is some evidence in the very bottom (core catcher area) of vibracores 15 (SAX04 site), 18, and 25 that denser, mottled, and ox-

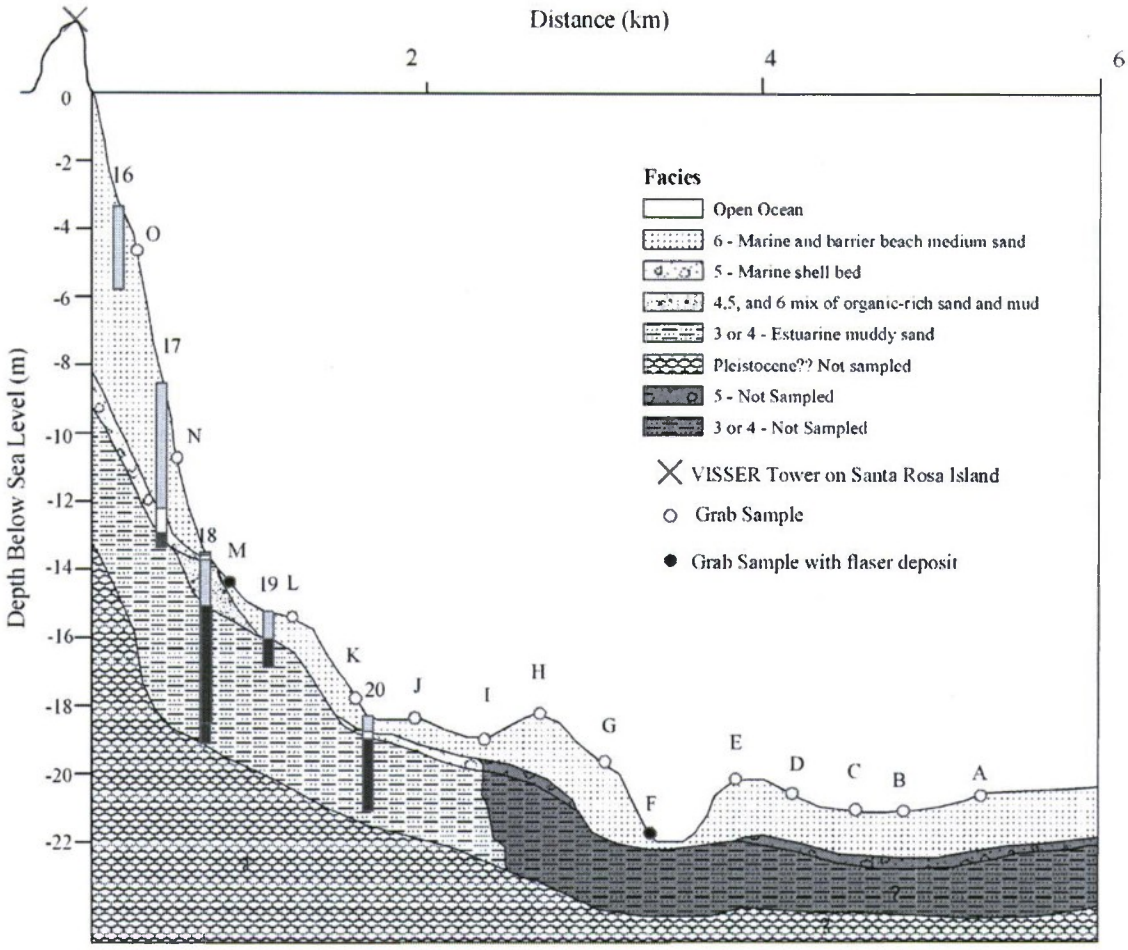

Fig. 11. VISSER tower vibracore and grab sample profile. Pattern fills indicate Facies. Facies numbers as described in text are indicated next to each pattern fill. Pleistocene units were not recovered in cores, but shown for visualization and estimated from previous work. Facies 3 and 4 were sampled nearest to shore, but depths of the facies are estimated farther offshore where only grab samples were collected. Vertical exaggeration = 200×.

idized sand might have been sampled, a description that fits the Pleistocene Prairie Formation at similar depths to these vibracores approximately 5–5.5 m bsf [19]. There are, however, not enough data collected in this study to support penetration of the Pleistocene units. It is possible that the denser Pleistocene units served to prevent further vibracore penetration before reaching maximum penetration.

V. Discussion

The shallow-water northwestern Florida Panhandle continental shelf offshore Santa Rosa Island is characterized by shore-oblique ridge-and-swale topography. The topography, superimposed on lower order Pleistocene morphologic features, is a strong control on sediment distribution in the near-shore environment. However, a discriminate depositional pattern follows strong storm events, such as Hurricane Ivan. Overall seafloor morphology of the region was created during Holocene and Pleistocene sea-level fluctuations. Storm-induced sedimentary and hydrodynamic processes have not only reworked the palimpsest shelf, but also maintained the shelf topography since the Wisconsinan sea-level lowstands. Accepted global "eustatic" sea-level curves associated with the Gulf of Mexico [53], [54] and a stratigraphic model along the Alabama/northwest Florida sand shelf [19] allow for basic reconstruction of the stratigraphy and depositional environment of the VISSER site based on vibracore interpretation. The following reconstruction is strongly influenced by [19], and extends those interpretations east into our study area.

Although radiocarbon dating and faunal assemblage analyses were not conducted, the vibracore samples likely did not penetrate into the Pleistocene units. Facies 5 and 6 together are up to 5.5 m thick, near the maximum penetration depth of the vibracorer system. The probable increase in density at the erosional surface, as well as another possible shell bed facies [19], would have resulted in core refusal. The Pleistocene units were deposited during the last global sea-level minimum associated with the late Wisconsinan glacial stage approximately 18 000 years B.P. when sea-level was more than 100 m below current sea level and fluvial and deltaic processes cut across the subaerially exposed shelf to the modern day shelf edge.

Sea-level rose rapidly (~0.9 cm/year) at the onset of the Wisconsinan glacial retreat, lasting approximately 7000 years and initiated a landward retreat of the shoreline. A slowdown in sea-level rise occurred around 11 000 yrs B.P. South Perdido Shoal, southwest of the study area at the 35-m isobath, is likely the former barrier shoreline position during this stillstand. The

Apalachicola River at that time cut across the shelf to the west of its present day location near the middle of the panhandle with a much higher discharge volume. The Choctawhatchee and Perdido Rivers also cut across the shelf with a higher discharge volume.

Sea-level rise recommenced at the onset of the Holocene epoch 10 000 years B.P. Facies 3 and 4, Holocene units that represent the deepest units sampled, are estuarine deposits of this early transgressive phase. The organic-rich, muddy shelly quartz sand, and associated wood and peat deposits, are indicative of a lower energy, subtidal environment, and represent the lower transgressive tract of an estuarine environment. Their deposition in a back-barrier lagoon or coastal embayment environment during the Holocene sea-level rise is further evident by the dark gray or green-laminated silt and clay layers being intermixed with shell-rich and fine- to medium-sand zones. Facies 3 and 4 were deposited in a partially enclosed estuarine environment influenced by marine processes. The sedimentary structure of these underlying facies has been maintained despite frequent high-energy storm events since emplacement.

Estuarine deposits appear closer to the seafloor surface in the bathymetric lows, as evident in vibracores 18, 20, and 25. Facies 6 is less extensive and the shell bed of Facies 5 is minimal. A gray sand or burnt-orange silty sand appeared deeper than 5 m bsf with mud inclusions and some signs of bioturbation. Thus, the upper portion of Facies 3 may be exposed here indicating an older estuarine deposit with rip-up clasts eroded from the mainland shoreline. This unit may have been deposited just before, or at the beginning of, the Holocene sea-level rise.

As sea-level rise continued episodically through to the mid-Holocene, the position of the lower Apalachicola River likely shifted to the east near its present day location. North Perdido Shoal, west–southwest of the study area at the 25-m isobath, is evidence of another standstill. Post-transgressive processes, such as tides, currents, and storm events, began to rework the sandy shelf when sea level neared its modern position likely 6000 to 3000 years B.P. [55]. The matrix-supported shell bed at the base of the Facies 6 sand unit formed as a transgressive lag deposit at the base of the shoreface in response to high-energy events. Subsequently, the shell bed was buried by sand deposition and reactivated by high-energy events that amalgamated younger, pristine shells into the layer. Facies 5 and 6 formed as the shelf was increasingly dominated by open marine environments, resulting in a sand deposit that is a combined 3.0–5.5-m-thick sand deposit. The modern seafloor of the Gulf has experienced a sea-level highstand ever since, and complete reworking of these upper transgressive systems tract is still occurring. Thus, Facies 5 and 6 are Holocene transgressive deposits reworked for the past 6000 years by post-transgressive hydrodynamic processes to form the shore-oblique surface sand ridges observed today.

Facies 6 comprises the barrier island shoreface and the shoreface-connected sand ridges of normal marine Gulf MAFLA sediments sourced from the eroding shoreface. These sediments were derived from alluvial sources during lower sea-level stands and redistributed by the E–W near-shore long-shore current and transport processes. Offshore sand is sourced from former shoreline features such as South and North Perdido Shoals, and reworked with rising sea levels. The near-shore shelf and beaches receive some of these sands, but most are sourced from upland watersheds and the southern Appalachian Mountains [19]. A line offshore Perdido Bay demarcates the Mobile Bay influence [19], which indicates that the VISSER/SAX04 sites are largely restricted from Mobile River sediments. Therefore, the Apalachicola River is still the major supplier of sand to the shelf in the study area due to the long-shore currents in the region. Contributions of sediments by the Perdido, Escambia, and Choctawhatchee Rivers are likely, considering their proximity to the study site.

The ridge-and-swale topography of the U.S. Atlantic shelf has been described as storm-generated current features [56]. The formation of this topography, applied to the barrier island shoreface and shoreface-connected sand ridge system along the northeastern Gulf shelf [18], [19], is also a result of these hydrodynamic processes and storm events. Troughs landward of the ridges undergo active scour and headward erosion in response to wind setup currents as described by [56]. The convergence of bottom currents as the wave-induced return flows through the troughs seaward causes ridge crest aggradation. Ridge detachment from the shoreface occurred during the Holocene transgression as the shoreface retreated landward, creating the present day near-shore continental shelf topography.

These processes continue along the modern day Gulf shelf and are evident in the seafloor. The thick sequence of Holocene sand on the ridges often thins landward of the ridges in the inter-ridge troughs. The wind and wave-generated (storm-generated) currents that maintain the ridge-and-swale topography prohibit or minimize the formation of the thick MAFLA sand sheet in the troughs, as evident from the persistence of this topography in before- and after-Ivan sidescan sonar imagery. Moreover, the ridge-and-swale topography is also evident in the stratigraphy of the vibracore samples: sedimentary structure formed during past depositional environments is maintained much nearer to the seafloor surface in the troughs than along the ridges. Silty, clayey, woody, and peaty layers, and elevated amounts of other organic material exist within the upper 0.5 m bsf with such material observed throughout the upper 5 m of the subbottom. Other areas of the subbottom exhibit this structure around 3 m bsf. The shell bed of Facies 5 is minimized or not evident at all within the swales, suggesting that reworking processes have obliterated this structure over time.

In fact, the upper 1.5 m of substrate along the barrier-shoreface trough contained a mix of sand, mud, and organic matter above the estuarine deposits of Facies 3 and 4. Wind- and wave-generated currents at the base of the barrier island shoreface acted to erode much of the sand sheet and allow sand and organic-rich, fine-grained material to mix together near the seafloor surface above the older sedimentary deposits.

The topography that controls storm-induced hydrodynamic and sediment transport processes does not create changes in sediment distribution following a major storm as much as it reinforces the existing morphology of the near-shore shelf. Relict sand, mobilized from the barrier shoreface or from offshore sand shoals, is redistributed along sand ridges as a result of the storm event. One result of the sediment redistribution is that sand is draped over much of the previously exposed hardbot-

toms. To a lesser degree, hardbottoms are revealed where previously buried, creating a collectively more extensive area of exposed hardbottoms poststorm despite being less apparent in individual areal extent in the sonar imagery. Sand is also draped over the edges of the mud swales, lessening their areal extent. Furthermore, mud swales have sharper demarcations and lack the prestorm diffuse boundaries, indicating deposition of fine-grained material in the troughs from current return flow and/or sand deposition along the swale edges. In this way, storm-induced hydrodynamic and sediment transport processes can be said to reinforce the existing ridge-and-swale topography.

Strong storms, such as Hurricane Ivan, can submerge barrier-island systems redistributing sand on shelf and introducing fine-grained material as sediment outflow from the bays and lagoonal areas. Although radionuclide and organic elemental results of offshore mud are inconclusive of their source, lignin–phenol gradients from Choctawhatchee Bay and from offshore mud samples indicate sediment outflow from the regional Gulf estuaries following Ivan. Furthermore, sediment outflow following storm events such as Ivan has been documented from MODIS imagery and other previous studies [5]–[8]. Examination of changes in grain shape distribution on the shelf following a 29-month period indicates that redistribution of sand is a continual process. The pattern of rougher, more angular grains offshore and more spherical grains onshore persists, though the grain shape population is slightly different due to grain sorting from winter storms and occasional regional tropical systems punctuating the relatively quiescent interval since Hurricane Ivan. It may be possible that the more spherical particles are still within the shelf's sand population, but sequestered into small-scale roughness features (ripple troughs) due to their propensity to migrate (roll down ripple faces) at low-energy conditions and the ability of ripples to migrate and bury trough sediments.

The low relief (<2 m) inter-ridge troughs tend to collect any fine-grained material in the system during storm interregnums, due to relatively quiescent hydrodynamic conditions. A storm event such as Ivan introduces additional fine-grained material to the system that concentrates in the NW–SE trending inter-ridge mud swales. Localized bathymetric lows along the shelf also act as depositional sinks for such remobilized fine-grained material that is subsequently covered over by migrating sand resulting in the formation of flaser deposits. The mud swales become better defined, and the shelf is dotted by mud "holes." Poststorm fine-grained deposition is clearly evident in the sonar imagery, the grab samples, and by diver observation.

Sediment transport processes continue to rework the shelf in the days and weeks following a storm. Wind–wave currents generate higher order ripple morphology over the MAFLA sand sheet. Sand is mobilized and draped across the newly deposited mud. Mud flaser deposits form, as observed in grab samples and diver observations. Flaser deposits are particularly present near bathymetric lows. However, wind- and wave-generated currents typically minimize or erode much of the fine-grained deposition along the shelf ridges maintaining the thick Facies 5 and 6 deposits of uniform medium sand of the MAFLA sand sheet while concentrating the fine-grained material in the inter-ridge mud swales. Thus, storm deposition or the introduction of new sediment to the palimpsest shelf acts along with the hydrodynamic forces to maintain the ridge-and-swale topography of the northeastern Gulf of Mexico near-shore continental shelf.

VI. Summary and Conclusion

Strong storms, such as Hurricane Ivan, serve to maintain the ridge-and-swale topography of the northeastern Gulf of Mexico continental shelf created during the Holocene transgression and controlled by present day hydrodynamic processes. Shelf topography controls sedimentary depositional patterns, including major depositional events following hurricanes and major storm events. Sand is typically deposited or aggraded onto sand ridges as a result of long-shore current flow and wave processes, whereas fine-grained material is deposited in the relatively quiescent environment of the inter-ridge troughs. Scour along the barrier island shoreface troughs landward of the ridge-and-swale topography minimizes the accumulation of the thick MAFLA sand sheet, and past sedimentary environments are revealed at shallow subsurface depths.

Following the passage of major storms, lagoonal outflow results in fine-grained deposition across the near-shore shelf. Hydrodynamic processes, controlled by continental shelf topography, dictate that inter-ridge troughs and localized bathymetric lows act as fine-grained depositional sinks. Sediment transport processes redistribute sand along the ridges and create a sand drape over the newly deposited soft mud in the localized bathymetric lows and form mud flaser deposits. These processes typically erode or minimize the distribution of the fine-grained material along shelf ridges in the days and weeks following a storm event, to be received by the inter-ridge troughs. Thus, the ridges are composed of thick ($\sim$ 5-m) uniform medium sand with higher order ripple morphology superimposed over the MAFLA sand sheet. The troughs serve as fine-grained sediment sinks. In this way, the ridge-and-swale topography is maintained.

Therefore, hurricanes, winter cold fronts, and other storm events serve to activate the northern Gulf of Mexico continental shelf by not only redistributing surficial relict sediments, but also by introducing new sediment to the shelf. Storm deposition onto the palimpsest shelf and reworking by the hydrodynamic forces of the near-shore environment act to maintain the ridge-and-swale topography of the northeastern Gulf of Mexico near-shore continental shelf rather than creating persistent major sedimentary event records or layers.

Acknowledgment

The authors would like to thank the crew of the *R/V Pelican* operated at LUMCON for their support in conducting the acoustic and grab sample surveys. N. DeWitt and R. Young of the U.S. Geological Survey (USGS), St. Petersburg, FL, and D. Bennett of Eckerd College, St. Petersburg, FL, made vibracore collection possible on the *R/V G.K Gilbert*. E. Dillon, T. Erman, and J. Watkins provided invaluable laboratory support. K. Yeager of the Department of Marine Sciences, University of Southern Mississippi, Hattiesburg, conducted the radiochemical and elemental analyses and R. Coffin of NRL, Washington, DC, provided the carbon isotope

analysis. E. Lee of Shell International Exploration and Production, New Orleans, LA, measured the sand friction angle and A. Falster of the Department of Geology, University of New Orleans, New Orleans, LA, provided the SEM images. B. Calder and B. Kraft of the Center for Coastal and Ocean Mapping, University of New Hampshire, Durham, provided multibeam data. R. Wheatcroft of Oregon State University, Corvallis, provided ^{7}Be radionuclide results for a sample collected immediately after hurricane Ivan. Finally, the authors would like to thank M. D. Richardson and T. Holland of NRL, Stennis Space Center, MS, for their support and advice.

REFERENCES

[1] H.-E. Reineck and I. B. Singh, *Depositional Sedimentory Environments*. New York: Springer-Verlag, 1980, p. 100 and 395.

[2] S. J. Bentley, T. R. Keen, C. A. Blain, and W. C. Vaughan, "The origin and preservation of a major hurricane event bed in the northern Gulf of Mexico: Hurricane Camille, 1969," *Mor. Geol.*, vol. 186, pp. 423–446, 2002.

[3] B. M. Velardo, S. J. Bentley, and G. W. Stone, "Impacts of tropical systems on the sedimentary fabric of the Mississippi Sound," *Trons. Gulf Coast Assoc. Geol. Soc. Gulf Coast Sect. SEPM*, vol. 53, pp. 815–823, 2003.

[4] T. R. Keen, S. J. Bentley, W. C. Vaughan, and C. A. Blain, "The generation and preservation of multiple hurricane beds in the northern Gulf of Mexico," *Mar. Geol.*, vol. 210, pp. 79–105, 2004.

[5] W. C. Isphording, D. Imsand, and G. C. Flowers, "Storm-related rejuvenation of a northern Gulf of Mexico estuary," *Trans. Gulf Coast Assoc. Geol. Soc. Gulf Coast Sect. SEPM*, vol. 37, pp. 357–370, 1987.

[6] W. C. Isphording and G. W. Isphording, "Identification of ancient storm events in buried Gulf Coast sediments," *Trons. Gulf Coost Assoc. Geol. Soc. Gulf Coast Sect. SEPM*, vol. 41, pp. 339–347, 1991.

[7] W. C. Isphording and F. D. Imsand, "Cyclonic events and sedimentation in the Gulf of Mexico," in *Coostol Sediments'91*, N. C. Kraus, K. J. Gingerich, and D. L. Kriebel, Eds. New York: ASCE, 1991, pp. 1122–1136.

[8] G. W. Stone, N. D. Walker, S. A. Hsu, A. Babin, B. Lui, B. D. Keim, W. Teague, D. Mitchell, and R. Leben, "Hurricane Ivan's impact along the Northern Gulf of Mexico," *EOS Trons. Amer. Geophys. Union*, vol. 86, no. 48, pp. 497–501, Nov. 2005.

[9] O. T. Marsh, "Geology of Escambia and Santa Rosa Counties, Western Florida Panhandle," *Florido Geol. Surv. Bull.*, vol. 46, pp. 4–9, 1966.

[10] L. J. Doyle and T. N. Sparks, "Sediments of the Mississippi, Alabama, Florida (MAFLA) continental shelf," *J. Sediment. Petrol.*, vol. 50, pp. 915–916, 1980.

[11] A. Goldstein, "Sedimentary petrologic provinces of the northern Gulf of Mexico," *J. Sediment. Petrol.*, vol. 12, pp. 77–84, 1942.

[12] T. H. Van Andel and D. M. Poole, "Sources of recent sediments in the northern Gulf of Mexico," *J. Sediment. Petrol.*, vol. 30, pp. 91–122, 1960.

[13] J. C. Ludwick, "Sediments in northeastern Gulf of Mexico," in *Papers in Morine Geology-Shepard Commemorative Volume*. New York: Macmillan, 1964, pp. 204–238.

[14] N. J. Hyne and H. G. Goodell, "Origin of the sediments and submarine geomorphology of the inner continental shelf off Choctawhatchee Bay, Florida," *Mor. Geol.*, vol. 5, pp. 299–313, 1967.

[15] S. D. Locker and L. J. Doyle, "Neogene to recent stratigraphy and depositional regimes of the northwest Florida inner continental shelf," *Mor. Geol.*, vol. 104, pp. 123–138, 1992.

[16] E. G. Otvos, "Santa Rosa Island, Florida Panhandle; origins of a composite barrier island," *Southeast. Geol.*, vol. 23, pp. 15–24, 1982.

[17] R. A. McBride, M. R. Byrnes, L. C. Anderson, and B. K. sen Gupta, "Holocene and Late Pleistocene sedimentary facies of a sand-rich continental shelf: A standard section for the northeastern Gulf of Mexico," *Trons. Gulf Coost Assoc. Geol. Soc. Gulf Coast Sect. SEPM*, vol. XLVI, pp. 287–299, 1996.

[18] R. A. McBride, "Seafloor morphology, geologic framework, and sedimentary processes of a sand-rich shelf offshore Alabama and Northwest Florida: Northeastern Gulf of Mexico," Ph.D. dissertation, Dept. Oceanogr. Coastal Sci., Louisiana State Univ., Baton Rouge, LA, 1997, unpublished.

[19] R. A. McBride, L. C. Anderson, A. Tudoran, and H. H. Roberts, "Holocene stratigraphic architecture of a sand-rich shelf and the origin of linear shoals: Northeastern Gulf of Mexico," in *Isolated Shollow Morine Sond Bodies: Sequence Stratigraphic Anolysis and Sedimentologic Interpretation*, K. M. Bergman and J. W. Snedden, Eds. Tulsa, OK: SEPM, 1999, vol. 64, Spec. Publ., pp. 95–126.

[20] R. A. McBride and T. F. Moslow, "Origin, evolution, and distribution of shoreface sand ridges, Atlantic inner shelf, U.S.A.," *Mor. Geol.*, vol. 97, pp. 57–85, 1991.

[21] S. J. Parker, A. W. Shultz, and W. W. Schroeder, "Sediment characteristics and seafloor topography of a palimpsest shelf, Mississippi-Alabama continental shelf," in *Quaternary Coasts of the United States: Marine and Lacustrine Systems*, C. H. Fletcher, III and J. F. Wehmiller, Eds. Tulsa, OK: SEPM, 1992, vol. 48, Spec. Publ., pp. 243–251.

[22] R. A. McBride and M. R. Byrnes, "Surficial sediments and morphology of the southwestern Alabama/western panhandle coast and shelf," *Trans. Gulf Coast Assoc. Geol. Soc. SEPM*, vol. XLV, pp. 393–404, 1995.

[23] H. N. Fisk and E. McFarlan Jr., "Late Quaternary deltaic deposits of the Mississippi River," in *Geol. Soc. Amer.*, 1955, pp. 279–302, Spec. Paper 62.

[24] J. Mazzullo and M. Peterson, "Sources and dispersal of Late Quaternary silt on the northern Gulf of Mexico continental shelf," *Mor. Geol.*, vol. 86, pp. 15–26, 1989.

[25] J. F. Donoghue, "Late Wisconsinan and Holocene depositional history, northeastern Gulf of Mexico," *Mar. Geol.*, vol. 112, pp. 185–205, 1993.

[26] K. J. Hsu, "Texture and mineralogy of the Recent sands of the Gulf Coast," *J. Sediment. Petrol.*, vol. 30, pp. 380–403, 1960.

[27] G. W. Stone, F. W. Stapor, J. P. May, and J. P. Morgan, "Multiple sediment sources and a cellular, non-integrated, longshore drift system: Northwest Florida and southeast Alabama coast, USA," *Mar. Geol.*, vol. 105, pp. 141–154, 1992.

[28] E. R. Foster, D. L. Spurgeon, and J. Cheng, "Shoreline change rate estimates: Escambia and Santa Rosa Counties," Florida Dept. Environ. Protection, Off Beach Coast. Syst., Tallahassee, FL, 1999, BCS-99-03.

[29] J. R. Abston, S. P. Dinnel, W. W. Schroeder, A. W. Shultz, and W. J. Wiseman Jr., "Coastal sediment plume morphology and its relationship to environmental forcing: Main Pass, Mobile Bay, Alabama," in *Coastal Sediments'87*, N. C. Kraus, Ed. New York: ASCE, 1987, pp. 1989–2005.

[30] W. C. Isphording, F. D. Imsand, and G. C. Flowers, "Physical characteristics and aging of Gulf Coast estuaries," *Trons. Gulf Coost Assoc. Geol. Soc. SEPM*, vol. XXXIX, pp. 387–401, 1989.

[31] R. P. Stumpf, "Observation of suspended sediments in Mobile Bay, Alabama from satellite," in *Coastal Sediments'91*, N. C. Kraus, K. J. Gingerich, and D. L. Kriebel, Eds. New York: ASCE, 1991, vol. 1, pp. 789–802.

[32] S. R. Stewart, "Tropical cyclone report: Hurricane Ivan, 2-24 September 2004," National Hurricane Center, Miami, FL, 2005 [Online]. Available: http://www.nhc.noaa.gov/2004ivan.shtml

[33] National Oceanic and Atmospheric Administration (NOAA), "Reports from the National Data Buoy Center's Stations in the Gulf of Mexico during the Passage of Hurricane Katrina," National Data Buoy Center (NDBC), Stennis Space Center, MS, 2006 [Online]. Available: http://www.ndbc.noaa.gov/hurricanes/2005/katrina/

[34] D. W. Wang, D. A. Mitchell, W. J. Teague, E. Jarosz, and M. S. Hulbert, "Extreme waves under Hurricane Ivan," *Science*, vol. 309, no. 5736, p. 896, 2005.

[35] B. J. Kraft and C. de Moustier, "Detailed bathymetric surveys offshore Santa Rosa Island, Florida: Before and after Hurricane Ivan (16 Sep. 2004)," *IEEE J. Oceon. Eng.*, 2010, to be published.

[36] R. L. Folk, *Petrology of Sedimentary Rocks*. Austin, TX: Hemphill, 1974, pp. 3–61.

[37] D. R. Jackson and M. D. Richardson, *High-Frequency Seafloor Acoustics*. New York: Springer-Verlag, 2007, pp. 201–222.

[38] R. F. Craig, *Soil Mechonics*. London, U.K.: Chapman & Hall, 1992, pp. 115–118.

[39] J. I. Hedges and J. R. Ertel, "Characterization of lignin by gas capillary chromatography of cupric oxide oxidation products," *Anal. Chem.*, vol. 54, pp. 174–178, 1982.
[40] M. A. Goni and J. I. Hedges, "Lignin dimers: Structures, distribution and potential geochemical applications," *Geochim. Cosmochim. Acta*, vol. 56, pp. 4025–4043, 1992.
[41] T. S. Bianchi, M. Arygyrou, and H. F. Chippett, "Contribution of vascular plant carbon to surface sediments across the coastal margin of Cyprus (eastern Mediterranean)," *Org. Geochem.*, vol. 30, pp. 287–297, 1999.
[42] T. S. Bianchi, S. Mitra, and B. A. McKee, "Sources of terrestrially-derived organic carbon in lower Mississippi River and Louisiana shelf sediments: Implications for differential sedimentation and transport at the coastal margin," *Mar. Chem.*, vol. 77, no. 2-3, pp. 211–233, 2002.
[43] K. V. Sarkanen and C. H. Ludwig, *Lignins-Occurrence, Formation, Structure and Reactions*. Cold Spring Harbor, NY: Wiley-Interscience, 1971.
[44] J. I. Hedges and D. C. Mann, "The characterization of plant tissues by their lignin oxidation products," *Geochim. Cosmochim. Acta*, vol. 43, no. 11, pp. 1803–1807, 1979.
[45] W. W. Schroeder, A. W. Shultz, and J. J. Dindo, "Inner-shelf hardbottom areas, northeastern Gulf of Mexico," *Trans. Gulf Coast Assoc. Geol. Soc. SEPM*, vol. XXXVIII, pp. 535–541, 1988.
[46] W. Schroeder, S. R. Gittings, M. R. Dardeau, P. Fleischer, W. W. Sager, A. W. Schultz, and R. Rezak, "Topographic features of the MAFLA continental shelf, northern Gulf of Mexico," in *Proc. IEEE OCEANS Conf.*, Seattle, WA, 1989, pp. 54–58, IEEE Publication Number 89CH2780-5.
[47] K. B. Briggs, A. H. Reed, D. R. Jackson, and D. Tang, "Fine-scale volume heterogeneity in storm-generated stratigraphy in sandy sediment off Fort Walton Beach, Florida, USA," *IEEE J. Ocean. Eng.*, 2010, to be published.
[48] D. R. Corbett, B. A. McKee, and M. A. Allison, "Nature of decadal-scale sediment accumulation in the Mississippi River deltaic region," *Continental Shelf Res.*, vol. 26, pp. 2125–2140, 2006.
[49] M. A. Goni, E. S. Gordon, N. M. Monacci, R. Clinton, R. Gisewhite, M. A. Allison, and G. Kineke, "The effect of Hurricane Lili on the distribution of organic matter along the inner Louisiana shelf (Gulf of Mexico, USA)," *Continental Shelf Res.*, vol. 26, pp. 2260–2280, 2006.
[50] S. Duan, T. S. Bianchi, A. M. Shiller, K. Dria, P. G. Hatcher, and K. R. Carman, "Variability in the bulk composition and abundance of dissolved organic matter in the lower Mississippi and Pearl rivers," *J. Geophys. Res.*, vol. 112, no. G02024, 2007.
[51] L. A. Wysocki, T. S. Bianchi, R. Powell, and N. Reuss, "Spatial variability in the coupling of organic carbon, nutrients, and phytoplankton pigments in surface waters and sediments of the Mississippi River plume," *Estuar. Coast. Shelf Sci.*, vol. 69, no. 1-2, pp. 47–63, 2006.
[52] T. P. Sampere, T. S. Bianchi, S. G. Wakeham, and M. A. Allison, "Sources or organic matter in surface sediments of the Louisiana Continental margin: Effects of primary depositional/transport pathways and a hurricane event," *Continental Shelf Res.*, to be published.
[53] R. G. Fairbanks, "A 17,000-year glacio-eustatic sea level record: Influence of glacial melting rates on the Younger Dryas event and deep-ocean circulation," *Nature*, vol. 342, pp. 637–642, 1989.
[54] R. G. Fairbanks, "The age and origin of the 'Younger Dryas climate event' in Greenland ice cores," *Paleoceanography*, vol. 5, pp. 937–948, 1990.
[55] D. J. P. Swift, "Response of the shelf floor to flow," in *Shelf Sands and Sandstone Reservoirs*, R. W. Tillman, D. J. P. Swift, and R. G. Walker, Eds. Tulsa, OK: SEPM, 1985, vol. 13, pp. 135–241.
[56] D. J. P. Swift, D. B. Duane, and T. F. McKinney, "Ridge and swale topography of the middle Atlantic Bight, North America: Secular response to the Holocene hydraulic regime," *Mar. Geol.*, vol. 15, pp. 227–247, 1973.

W. Chad Vaughan received the B.S. degree in geology from Furman University, Greenville, SC, in 1997 and the M.S. degree in geology from the University of New Orleans, New Orleans, LA, in 1999.

He began working at the U.S. Naval Research Laboratory, Stennis Space Center, MS, as a graduate student in 1998 studying the effects of bioturbation on the structure and permeability of fine-grained estuarine sediments. He has participated in various investigations of sediment physical and geotechnical properties of the seafloor while at the Naval Research Laboratory until 2008. He is currently a Geologist at the Minerals Management Service, New Orleans, LA, identifying, mapping, and evaluating petroleum reservoirs in the Gulf of Mexico.

Mr. Vaughan is a member of the American Geophysical Union and the New Orleans Geological Society.

Kevin B. Briggs received the B.S. degree in biology from Florida Atlantic University, Boca Raton, in 1975, the M.S. degree in zoology from the University of Georgia, Athens, in 1978, and the Ph.D. degree in marine geology and geophysics from the Rosenstiel School of Marine and Atmospheric Science, University of Miami, Miami, FL, in 1994.

He began working at the Naval Ocean Research and Development Activity, now part of the U.S. Naval Research Laboratory (NRL), at the Stennis Space Center, MS, in 1979, where he was involved in research on the effects of environmental processes on sediment geoacoustic properties. He has participated in many shallow-water high-frequency acoustics experiments as an investigator of geoacoustic and roughness properties of the seafloor. He is currently engaged in research on characterization of sediment interface roughness and volume heterogeneity for high-frequency acoustic modeling. He has over 40 published articles on physical and acoustic properties of the sea floor.

Dr. Briggs is a member of the Acoustical Society of America, the American Geophysical Union, and Sigma Xi.

Jin-Wook Klm received the B.S. degree from Yonsei University, Seoul, Korea, in 1989, the M.S. degree from University of Michigan, Ann Arbor, in 1994, and the Ph.D. degree from Texas A&M University, College Station, in 1999, all in geology.

Currently, he is a Professor at Yonsei University. His research experience of eight years as a Geologist at the U.S. Naval Research Laboratory, Stennis Space Center, MS, was preceded by four years of research scientist as a Mineralogist at Texas A&M University. His research has concentrated on clay–microbe interaction, sealing rock characterization, and shale diagenesis.

Thomas S. Bianchi received the B.A. degree in biology with a minor in chemistry from Dowling College, Long Island, NY, in 1978, the M.S. degree in ecology and evolution from the State University of New York (SUNY), Stony Brook, in 1981, and the Ph.D. degree in marine sciences–biogeochemistry from the University of Maryland, College Park, in 1987.

His areas of expertise are organic geochemistry, biogeochemical dynamics of aquatic food chains, and carbon cycling in estuarine and coastal ecosystems. When on a Fulbright Scholarship in Sweden, at the Stockholm University, he was involved in projects that examined the effects of changing redox on the decay dynamics of organic matter in sediments, and the paleo-reconstruction of cyanobacterial blooms in the Baltic Sea. On another Fulbright in Cyprus, he worked on organic carbon cycling coastal water. His most recent award was the William Evans Fellowship, Research Scholar (2007), Otago University, New Zealand, where he spent time in New Zealand giving lectures and coordinating research projects. He has published over 93 articles in refereed journals and was lead co-editor (Bianchi, Pennock, and Twilley) of a book entitled *Biogeochemistry of Gulf Mexico Estuaries* (New York: Wiley, 1999), and a new sole-authored book entitled *Biogeochemistry of Estuaries* (Oxford, U.K.: Oxford Univ. Press, 2007). He is also currently half-way through a new book entitled *Chemical Biomarkers in Aquatic Ecosystems* by Bianchi and Canuel (Princeton, NJ: Princeton Univ. Press, 2009).

Dr. Bianchi currently serves as an Associate Editor for the journals *Marine Chemistry*, *Organic Geochemistry*, *Geochimica et Cosmochimica Acta*, and *Marine and Freshwater Systems*. He has served on many advisory committees and professional societies have been as a reviewer for numerous journals and funding agencies.

Richard W. Smith received the B.S. degree in chemistry as well as aquatic ecology from SUNY Brockport, Brockport, NY, in 2007. He is currently working towards the Ph.D. degree at the Oceanography Department, Texas A&M University, College Station, under Dr. T. S. Bianchi.

His dissertation work involves using lignin and lipid biomarkers, including the branched/isoprenoid tetraether (BIT) index, to look at changes in terrestrial organic matter transport to Fjordland, New Zealand, in the recent anthropocene as it relates to climate change. He has also worked on numerous projects including the contribution of terrestrial organic matter to hypoxia in the Gulf of Mexico, and changes in the quality of carbon delivered to San Francisco Bay, as it relates to land use. He has also done numerous projects at the Gerace Research Station, San Salvador, The Bahamas, including hypersaline lake hydrology, and mangrove juvenile fish abundance as part of a marine sanctuary project.

Mr. Smith is a member of the American Chemical Society, and the American Society of Limnology and Oceanography.